

20,870  
ASD TECHNICAL REPORT 61-278  
SUPPLEMENT 2

IV  
AFML TECHNICAL LIBRARY  
OFFICIAL FILE COPY.

REVIEW OF FIRE AND EXPLOSION HAZARDS  
OF FLIGHT VEHICLE COMBUSTIBLES  
(Supplement 2)

HENRY E. PERLEE  
ISRAEL. LIEBMAN  
MICHAEL G. ZABETAKIS

BUREAU OF MINES  
UNITED STATES DEPARTMENT OF THE INTERIOR

APRIL 1963

AERONAUTICAL SYSTEMS DIVISION

## NOTICES

When Government drawings, specifications, or other data are used for any purpose other than in connection with a definitely related Government procurement operation, the United States Government thereby incurs no responsibility nor any obligation whatsoever; and the fact that the Government may have formulated, furnished, or in any way supplied the said drawings, specifications, or other data, is not to be regarded by implication or otherwise as in any manner licensing the holder or any other person or corporation, or conveying any rights or permission to manufacture, use, or sell any patented invention that may in any way be related thereto.

Qualified requesters may obtain copies of this report from the Armed Services Technical Information Agency, (ASTIA), Arlington Hall Station, Arlington 12, Virginia.

This report has been released to the Office of Technical Services, U. S. Department of Commerce, Washington 25, D. C., for sale to the general public.

Copies of ASD Technical Reports and Technical Notes should not be returned to the Aeronautical Systems Division unless return is required by security considerations, contractual obligations, or notice on a specific document.

REVIEW OF FIRE AND EXPLOSION HAZARDS  
OF FLIGHT VEHICLE COMBUSTIBLES  
(Supplement 2)

HENRY E. PERLEE  
ISRAEL LIEBMAN  
MICHAEL G. ZABETAKIS

BUREAU OF MINES  
UNITED STATES DEPARTMENT OF THE INTERIOR

APRIL 1963

Delivery Order AF (33-616) 60-8  
Project No. 6075  
Task No. 607504

AERO PROPULSION LABORATORY  
AERONAUTICAL SYSTEMS DIVISION  
AIR FORCE SYSTEMS COMMAND  
WRIGHT-PATTERSON AIR FORCE BASE, OHIO

## FOREWORD

This report was prepared by the Explosives Research Center of the U. S. Bureau of Mines, under USAF Delivery Order (33-616) 60-8, Project No. 6075, "Flight Vehicle Hazard Protection", Task No. 607504, "Fire and Explosion Characteristics of Aerospace Vehicle Combustibles". It was administered under the direction of the Aeronautical Systems Division, Wright-Patterson Air Force Base, with Mr. Benito Botteri as project engineer. The report covers work done during the period April 1962 to April 1963 and is the third annual report on this contract.

## ABSTRACT

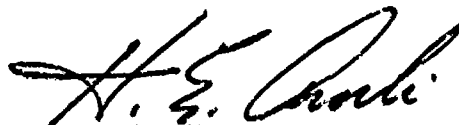
This is the third in a series of reports on the fire and explosion hazards associated with combustibles and other gases likely to be found in aircraft and missile systems. It presents theoretical and experimental results on homogeneous and heterogeneous mixtures in air.

Two pressure peaks were observed in venting hydrogen-air mixtures into a low pressure atmosphere. When venting a fire above a liquid pool under the same conditions, the liquid regression rate and flame size were found to increase.

Molecular diffusion appears to be the chief factor in establishing the position of the lower limit of flammability of both lighter-than-air and heavier-than-air combustible, quiescent, gas layers; the position of the upper limit cannot be predicted by considering molecular diffusion alone.

The ratio of the work done against the gravitational force to that done by the turbulent stresses is useful in analyzing mixing processes in flowing, layered systems. The gravitational field strength also appears to affect the time delay before ignition of a combustible vapor in air.

This report has been reviewed and is approved.



H. E. AMLI  
Chief, Support Techniques Division  
AF Aero Propulsion Laboratory

## TABLE OF CONTENTS

	<u>Page</u>
INTRODUCTION .....	1
RESULTS AND DISCUSSION .....	2
Homogeneous Mixtures .....	2
Heterogeneous Mixtures .....	2
Quiescent Atmospheres .....	2
Mixing rate .....	2
Flammability .....	3
Nonquiescent Atmospheres .....	5
Mixing rate .....	5
Flame propagation .....	7
Burning Pools .....	8
Low rate of pressure change .....	8
High rate of pressure change .....	9
Autoignition in Accelerated Fields .....	10
SUMMARY AND CONCLUSIONS .....	11
PROPOSED INVESTIGATIONS .....	12
REFERENCES .....	13
APPENDIX I - Low Pressure Chamber .....	38
APPENDIX II - Quiescent Stratified Mixtures (Large Concentration Gradients) .....	41
APPENDIX III - Quiescent Stratified Mixtures (Small Concentration Gradients) .....	44
APPENDIX IV - Flowing Stratified Mixtures ....	46
APPENDIX V - Acceleration Apparatus .....	48

# LIST OF ILLUSTRATIONS

<u>Figure</u>		<u>Page</u>
1.	Pressure trace produced following the ignition of a uniform hydrogen-air mixture in a vented enclosure .....	14
2.	Pressure traces produced following the ignition of a uniform hydrogen-air mixture containing 13 volume percent hydrogen for various external vent pressures .....	15
3.	Concentration profiles of methane diffusing downward into air for a homogeneous methane-air mixture with an initial concentration $C_0$ and an initial depth $l$ .....	16
4.	Pressure records obtained during the combustion of stratified layers of methane-air and pentane-air mixtures in air after a diffusion time of 2 minutes .....	17
5.	Maximum pressures developed during the combustion of stratified layers of methane-air mixtures in air for various diffusion times, and initial methane concentrations, $C_0$ .....	18
6.	Maximum pressures developed during the combustion of stratified layers of pentane-air mixtures in air for various diffusion times, and initial pentane concentrations, $C_0$ .....	19
7.	Range of flammable mixture compositions formed from the diffusion of methane into air at 75° F .....	20
8.	Range of flammable mixture compositions formed from the diffusion of pentane into air at 75° F .....	21
9.	Position of flame front along a vertical 4-inch tube following ignition of two heterogeneous and one homogeneous methane-air mixtures at atmospheric pressure and 75° F .....	22
10.	Flame speeds through homogeneous and heterogeneous methane-air mixtures in 4-inch cylindrical tubes at atmospheric pressure and ambient temperature .....	23
11.	Concentration of natural gas as a function of distance from the gallery roof, 6-2/3 feet downstream from the gas inlet for a natural gas inlet flow of 5 ft <sup>3</sup> /min and ventilating velocities of 80, 100 and 140 ft/min .....	24

# LIST OF ILLUSTRATIONS (Con)

<u>Figure</u>		<u>Page</u>
12.	Concentration of natural gas as a function of distance from the gallery roof, 6-2/3 feet downstream from the gas inlet for a natural gas inlet flow of 17 ft <sup>3</sup> /min and ventilating velocities of 80, 100 and 140 ft/min .....	25
13.	Concentration of natural gas at the gallery roof as a function of distance from the natural gas inlet (diffuser outlet) for natural gas flow of 5 ft <sup>3</sup> /min showing the effect of ventilation velocity .....	26
14.	Concentration of natural gas at the gallery roof as a function of distance from the natural gas inlet (diffuser outlet) for natural gas flow of 17 ft <sup>3</sup> /min showing the effect of ventilation velocity .....	27
15.	Concentration of carbon dioxide gas at the gallery floor level as a function of distance from the carbon dioxide inlet showing the effect of ventilating velocity .....	28
16.	Concentration of carbon dioxide gas at the gallery floor level as a function of distance from the carbon dioxide inlet showing the effect of variation in CO <sub>2</sub> diffuser outlet design .....	29
17.	Concentration of carbon dioxide gas at the gallery floor level as a function of distance from the carbon dioxide inlet, showing the effect of baffle plates placed on the tunnel floor .....	30
18.	Two sets of successive frames from motion picture sequence (16 frames/sec) of a flame propagating through a natural gas-air layer in a 6.5 ft-diameter gallery .....	31
19.	Radiant energy received by photodiodes on the gallery floor following passage of flame through natural gas-air layers along the roof .....	32
20.	Effects of natural gas flow rate, ventilation velocity, and location of ignition source on the flame velocity through stratified natural gas-air layers in a 6.5-ft diameter gallery .....	33
21.	Photographs of wax candle flame burning in air at various pressures .....	34



# LIST OF ILLUSTRATIONS (Con)

<u>Figure</u>		<u>Page</u>
22.	Liquid regression rate of burning pools of UDMH and JP-6 in one-inch diameter trays as a function of environmental pressure .....	35
23.	Pressure histories following (a) venting a 24-inch diameter sphere at 15 psia pressure into a low pressure environment (0.01 psia), (b) venting the same sphere containing a burning pool of liquid UDMH and (c) venting a gas phase explosion of gasoline vapors in air .....	36
24.	Autoignition time delays of n-decane in 5-inch diameter stainless steel spherical vessels at 417° F for accelerational fields of 1 g and 10 g .....	37
25.	Twelve-foot low pressure environment sphere .....	39
26.	Two-foot diameter test sphere .....	40
27.	Apparatus used in quiescent stratification experiments .....	42
28.	Lower portion of sphere used in stratification experiments..	43
29.	Schema of apparatus used to prepare heterogeneous methane-air mixtures .....	45
30.	Gallery and associated apparatus used for flammability studies of flowing mixtures .....	47
31.	Acceleration apparatus .....	49

## INTRODUCTION

This is the third annual report on the fire and explosion hazards associated with combustibles used in aircraft and missile systems. It gives a summary of the mixing, explosion pressure, venting and autoignition data obtained here during the past year. The first two reports (refs. 1 and 2) presented a general discussion of fire and explosion phenomena and included vapor pressure and flammability characteristics data for a number of combustibles and oxidants.

Homogeneous mixtures have been considered in most flammability studies conducted in the past. Although such mixtures are also considered here, most of the present study is devoted to heterogeneous mixtures since these invariably result when a combustible leaks into a confined space under quiescent and flowing conditions. Both lighter-than-air and heavier-than-air gases have been investigated. Layering and combustion experiments were conducted with methane and pentane in air, and layering experiments with carbon dioxide in air. In addition, venting experiments were conducted with uniform hydrogen-air mixtures; burning studies were conducted with liquid fuels at reduced pressures; autoignition experiments were conducted to determine the effects of the gravitational field strength on the autoignition characteristics of fuel vapor-air mixtures.

---

Manuscript released by authors May 1963 for publication as an ASD  
Technical Documentary Report.

## RESULTS AND DISCUSSION

### Homogeneous Mixtures

When a deflagration is initiated in an unvented enclosure, the pressure rises to a maximum value and then falls slowly as the combustion gases cool. The pressure rise at any time  $t$  following ignition is proportional to the cube of  $t$ . However, if the flame contacts a cold surface or an inhibitor, the pressure rise rate decreases. In a vented enclosure, the pressure rise rate is influenced by the nature and mode of operation of the vent. A few preliminary venting experiments were conducted with uniform hydrogen-air mixtures at an initial pressure of one atmosphere. The apparatus which is described more fully in Appendix I consists of a 2-foot sphere enclosed in a 12-foot vacuum sphere. A typical pressure trace obtained following ignition of a hydrogen-air mixture is shown in Figure 1. The pressure is observed to rise from the initial value  $P_0$  (1 atmosphere) to a value  $P_1$ , fall suddenly, rise again to a value  $P_2$ , and then fall rapidly to the final ambient subatmospheric pressure  $P_f$ ; the 4-inch vent functioned at the instant  $t_v$ . Two pressure peaks were observed in the venting experiments conducted at atmospheric and reduced environmental pressures  $P_f$ . Similar results have been reported by Simmonds and Cabbage (refs. 3, 4, and 5) who investigated the design of effective vents for industrial drying ovens operated at atmospheric pressure.

The pressure traces obtained with 13 volume percent hydrogen-air mixtures at 80° F and one atmosphere initial pressure are given in Figure 2. Without the 4-inch vent, a maximum pressure of 70 psi was attained; the maximum pressure ( $P_2$ ) was 45 psi when the 4-inch vent was used at an ambient (environmental) pressure of one atmosphere, and 28 psi when it was used at 0.5 and 0.03 atmosphere. The initial pressure pulse ( $P_1$ ) was lower than  $P_2$  in each case. It appears that  $P_1$  may be reduced for any given volume by the use of a vent diaphragm of small inertia that functions at lower pressures;  $P_2$  may be reduced by the use of a larger vent opening (refs. 3, 4, and 5).

### Heterogeneous Mixtures

#### Quiescent Atmospheres

##### Mixing Rate. -

When a combustible gas or vapor leaks slowly into a quiescent atmosphere, it mixes with the atmosphere by one or more of the following mechanisms: molecular diffusion; natural convection; forced convection. In the absence of a gravitational field, or where convection effects can be ignored, mixing occurs primarily by molecular diffusion when the leak rate is very slow. For example, this occurs in a uniform temperature environment in a gravitational field when a lighter-than-air gas is released near the roof or when a heavier-than-air gas is released near the base of an enclosure.

The concentration profiles obtained when methane-air mixtures are permitted to diffuse downward into air in a cylinder at 1, 2 and 5 minutes are given in Figure 3;  $C$  is the methane concentration at any position  $y$ ,  $C_0$  is the initial concentration, and  $l$  is the initial layer depth (1.5 inches in this case). The concentration profiles were calculated with the aid of an analog computer. A diffusion coefficient of  $1.46 \text{ in}^2/\text{min}$  (ref. 6) was taken for methane. A similar calculation was made for pentane-air mixtures diffusing upward into air. The concentration profiles were similar to those given in Figure 3 with the diffusion times (1, 2 and 5 minutes) increased by a factor of about 4.5; a diffusion coefficient of  $0.324 \text{ in}^2/\text{min}$  (ref. 7) was taken for pentane.

As an example in the use of Figure 3, consider a layer of pure methane ( $C_0 = 100\%$ ). Approximately 5 minutes would be required to reduce the concentration of methane at the top of a 1.5-inch deep enclosure to the stoichiometric value (about 9.5%). Approximately 22 minutes would be required to reduce the pentane concentration to 9.5 percent at the bottom of a similar inverted enclosure that contained pure pentane initially; an even longer interval would be required to reduce the concentration to the stoichiometric value (about 2.6%), or to the lower limit of flammability at atmospheric pressure and  $80^\circ \text{ F}$  (1.4%).

#### Flammability. -

Pressure records such as those given in Figure 4 are obtained by the ignition of the heterogeneous mixtures formed from the diffusion of a combustible gas in air. In each case, 4.7 cubic inches of homogeneous combustible-air mixture was permitted to diffuse into 260 cubic inches of air via a short cylindrical chamber (Appendix II), for 2 minutes before ignition. (The vertical dotted line in Figure 3 corresponds to the location of the ignition source). Pentane-air mixtures with initial compositions ( $C_0$ ) within or near the flammable range burned rather smoothly; however, mixtures with initial pentane concentrations considerably above the upper limit of flammability produced pressure oscillations as shown in Figure 4 for  $C_0 = 21$  percent. Such pressure oscillations were not observed with any of the methane-air mixtures used. A plot of the maximum pressures obtained in this study for various initial combustible concentrations and diffusion times are given in Figures 5 and 6 for methane and pentane, respectively. These figures show that as the diffusion times increase, the initial range of mixture compositions that forms flammable mixtures in this apparatus also increases, that is, the apparent (apparatus dependent) "limits of flammability" are widened. Further, the largest maximum pressures obtained from the data given in Figures 5 and 6 are in the range 2.5 to 3 psi. If this pressure range is multiplied by the ratio of the total volume of the apparatus ( $260 \text{ in}^3$ ) to the initial volume of the homogeneous gas mixture ( $4.7 \text{ in}^3$ ) a pressure range of 140-160 psi is obtained. These pressures are in the neighborhood of the maximum pressure developed with a homogeneous stoichiometric methane-air mixture (about 130 psi).

Ideally, a flame should not propagate through a homogeneous vapor-air mixture if the combustible vapor concentration in the vicinity of the ignition source is below the lower limit or above the upper limit of flammability. Assuming this to be true and using the curves given in Figure 3, calculated upper and lower limit-of-flammability curves can be obtained as a function of diffusion time; these are given in Figures 7 and 8 for the combustible vapor-air layers considered here. Also shown in these figures are the experimental limits obtained from Figures 5 and 6. The vertical lines at each point are a measure of the experimental scatter in the data. The lower limit experimental and calculated curves show satisfactory agreement in each case; however, the corresponding curves for the upper limits show considerable deviation. This is to be expected since even for homogeneous mixtures whose combustible composition is above the upper limit, a flame will, in general, propagate a short distance away from the ignition source before it is extinguished. Therefore, for the concentration gradients tested here, it is only necessary for the flame or hot gases to propagate away from the ignition source about one inch before it will encounter a flammable mixture. However, as the diffusion times increase the concentration gradients decrease and the calculated and experimental upper limit curves should eventually merge.

The burning characteristics of heterogeneous combustible-air systems characterized by small concentration gradients have been determined in a 4-inch diameter, 8-foot long Plexiglas tube. The tube was filled with a heterogeneous methane-air mixture whose composition varied linearly from 5 percent methane at the bottom to 20 percent methane at the top; such mixtures were prepared with the apparatus described in Appendix III. The mixture compositions listed along the right-hand ordinate (Figure 9) are those corresponding to the locations along the left-hand ordinate. These mixtures were ignited at the bottom of the tube by means of an electrically heated wire and a small quantity of guncotton. The propagation of the flame up the tube was photographed with a motion picture camera operating at 64 frames per second. The position of the flame front on the developed film was then read with a traveling microscope. The results of these experiments are shown in Figure 9 where the flame position is plotted as a function of time elapsed after the onset of ignition. The apparently high initial flame speed indicated in the figure for the heterogeneous systems is virtual since, when the guncotton ignites, incandescent particles are thrown up the tube igniting the gas mixture some inches from the actual location of the hot wire. Also shown in the figure is the corresponding curve for a flame traveling through a homogeneous mixture of 8.4 volume percent methane in air. The flame speeds obtained from the photographic records are given in Figure 10. This figure also includes flame speed data obtained by Coward and Hartwell (ref. 8) for homogeneous gas mixtures in a 4-inch horizontal pipe. Since flame speeds in horizontal pipes are lower than those in vertical pipes, the results shown in Figure 10 for the homogeneous mixtures of Coward and Hartwell and heterogeneous mixtures in this research are consistent and in satisfactory agreement. These results indicate that flame speed is a function of combustible concentration and is apparently independent of the flame's previous history.

## Nonquiescent Atmospheres

### Mixing Rate. -

The turbulent mixing of two moving fluids of different densities has been analyzed by Richardson (ref. 9) in terms of the following equation:

$$Ri = \frac{g}{\rho} \frac{\delta \rho}{\delta y} \bigg/ \left( \frac{\delta u}{\delta y} \right)^2 \quad (1)$$

where  $Ri$  is the Richardson number,  $g$  is the gravitational constant,  $\rho$  is the fluid density,  $\delta \rho / \delta y$  and  $\delta u / \delta y$  are the density and velocity gradients across the fluid boundary. This expression is a ratio of the work done against gravity to that done by the turbulent stresses. If the turbulent stresses are large enough (low  $Ri$  number), mixing of the two fluids will occur; otherwise (large  $Ri$  number) a stable layer results. Density and velocity gradients change across the layer so that the factors of equation 1 are difficult to specify; however, the following approximation can be employed:

$$Ri = \frac{\delta(\rho_a - \rho_g)h}{\rho_a} \bigg/ (U - v)^2 \quad (2)$$

where  $\rho_a$  and  $U$  are the density and velocity of the ventilation air adjacent to the layer edge, and  $\rho_g$ ,  $h$ , and  $v$  are the averaged density, height, and velocity of the layer. Similar forms of this equation have been used by Ellison (ref. 10) and by Bakke (ref. 11).

For an evaluation of equation 2, natural gas-air strata were first studied. Experiments were carried out in a horizontal metal cylinder 67 feet long and 6-1/2 feet in diameter (Appendix IV). A fan with a blade diameter of 2-1/4 feet, driven by a 5-hp motor, was placed at one end of this tunnel or gallery. Air flow was controlled by varying the motor speed and by placing screens on the intake side of the fan. The natural gas was piped at a constant flow rate through the tunnel roof to a diffuser located 26 feet from the fan. The diffuser consisted of a 1/2-inch thick piece of flat plywood, 7 feet long with tapered sides. When supported against the inner roof, the diffuser permitted the development of a 3-foot wide layer of pure natural gas along the roof. The natural gas concentration was determined by probing through the tunnel roof at four equidistant stations, the first being 6-2/3 feet downstream from the diffuser outlet. The gas samples were analyzed with a thermal conductivity analyzer. Air ventilation velocities were determined with a hot-wire anemometer.

Gas concentration profiles measured at the first sampling station with natural gas flow rates of 5 and 17 ft<sup>3</sup>/min are shown in Figures 11 and 12. In Figures 13 and 14 are shown the roof concentrations at various distances from the gas inlet for natural gas flow rates of 5 and 17 ft<sup>3</sup>/min. Using

the profiles of Figures 11 and 12, the unknowns of equation 2 are determined by calculating the cross-sectional area,  $A_m$ , occupied by pure natural gas, and the total layer cross section. The layer velocity,  $v$ , is obtained from the continuity equation for natural gas,  $vA_m = V$ , where  $V$  is the natural gas volume flow rate. The  $Ri$  numbers obtained in this manner are shown in Figures 13 and 14; these are averaged values obtained from the four sampling stations. Ellison, (ref. 10) who investigated turbulent buoyant plumes, found that turbulent entrainment in the layer became negligible when  $Ri$  exceeded 0.8. From Figure 14, mixing is indeed small for  $Ri \geq 1.2$ , although it should be noted that upstream of the first station, some mixing occurs for all ventilation velocities studied. Within this region (upstream of the first station) the slow moving natural gas layer accelerates, finally attaining a constant velocity over the remaining layer length. For  $Ri = 0.4$ , Figures 13 and 14 show that the natural gas concentration at the roof drops to the lower flammable limit (about 5 percent methane) within approximately 35 feet from the natural gas inlet.

To obtain the mixing characteristics of a heavier-than-air gas, data were obtained for a carbon dioxide-air stratum. To simulate flow conditions on a flat surface, the previously described tunnel or gallery was modified to include a four foot wide plywood floor extending its entire length. The carbon dioxide was admitted at floor level by means of a diffuser below the floor. The rectangular diffuser outlet was of the same width as the floor and either 1/2 or 1-1/2 feet in length.

The carbon dioxide concentrations at floor level, measured both upstream and downstream from the gas inlet, are shown in Figure 15 for the 1-1/2-foot long diffuser and for main air stream velocities of 120 and 160 feet/min. From Figure 15 it can be seen that the Richardson criterion is apparently valid for layers of the heavier-than-air gas considered here. Figure 15 shows carbon dioxide was found upstream of the inlet for both of the ventilation velocities investigated. This upstream flow of carbon dioxide increases the velocity of the carbon dioxide layer relative to that of the main air stream and therefore, according to Richardson's criterion, should enhance mixing.

The concentration of carbon dioxide at floor level, measured upstream and downstream from the gas inlet, is shown in Figure 16 for a ventilating flow velocity of 120 ft/min (approximately 2900 ft<sup>3</sup>/min) and a carbon dioxide volumetric flow rate of 15 ft<sup>3</sup>/min for three different outlet configurations. Curves A and B of Figure 16 correspond to diffuser outlet openings mounted flush with the floor and having 1/2 and 1-1/2-foot lengths. These curves show that reducing the diffuser opening by a factor of one third apparently has little effect on the mixing characteristics of these stratified layers. Curve C in the same figure shows the results obtained when the diffuser outlet was covered by an inclined lid whose upstream edge was flush against the floor and whose downstream edge was raised 1/4-foot

above the floor level. This arrangement permitted the carbon dioxide to leave the diffuser with an initial velocity downstream and none upstream. In accordance with Richardson's criterion, the degree of mixing was decreased when this inclined lid was used (compare curves A and C). Measurements were made to determine the influence of short (1/2-ft high) baffles in the mixing of carbon dioxide-air layers. The baffles were placed on the floor extending the width of the tunnel. Figure 17 shows the results obtained with carbon dioxide-air layers using the 1-1/2-ft long diffuser outlet and ventilating flow velocities of 120 ft/min. The letters labeling the curves in this figure refer to the positions of the baffles as indicated on the abscissa. For comparison, results obtained without a baffle are shown by the curve N. Curve A represents the results obtained with a baffle immediately upstream of the diffuser outlet. The figure shows that a baffle in this location eliminates any upstream flow of carbon dioxide. Comparison of these results with those where upstream flow is present, curve N, appears to further substantiate the conclusion that upstream flow enhances mixing. Further, curve A of Figure 17 is very similar to curve C of Figure 16 where no upstream flow exists. Introducing an additional baffle immediately ahead of the diffuser, curve A,B, shows that mixing is appreciably increased when compared with the case when only one baffle (A) is used, although mixing is not much better than for the situation with no baffles at all. Further, moving this latter baffle three feet downstream increases the mixing as shown by curve A,C. Removing the upstream baffle, thereby permitting upstream flow, results in still greater mixing as shown by curve C. Layer entrainment due to eddy formation produced by the baffles is comparatively negligible as seen by the relatively large downstream concentration of curves A and A,B and the large concentration difference between curves A,B and A,C.

#### Flame Propagation. -

With the initial experimental arrangement, natural gas-air roof layers were ignited and the resulting flame velocities and flame radiation were measured. Ignition was achieved with electric match heads fixed near the tunnel exit. The flame therefore propagated with or against the layer flow. A 16 mm movie camera placed 6 feet from the tunnel exit was focused on the tunnel roof and contained a field of view from the natural-gas inlet to within 7 feet of the tunnel exit. Figure 18 shows flame photographs taken in this manner. The left side shows a flame propagating downstream 2 seconds after ignition, the right side shows the occurrence of afterburning following the initial flame passage.

Four photodiode cells were placed on the tunnel floor spaced 6-2/3 feet apart. Encased in a box with an aperture, each cell viewed only a 7.3 ft<sup>2</sup> portion of the overhead flame. The radiant energy measured by these cells is shown in Figure 19. From this figure the flame length near peak flame luminosity is approximately 10 feet long which would result in a maximum transfer of radiant energy to the tunnel floor of 0.01 cal/cm<sup>2</sup> sec. This



is roughly 0.5 percent of the level necessary to give second degree burns. Flame velocities were determined from movie film showing the flare of gun-cotton pieces placed at equi-distant stations near the tunnel roof and from the distance between recorded radiation peaks (Figure 19). The averaged flame velocities are shown in Figure 20. In the lower portion of this graph the flame velocities are uniform and show a decreased velocity in propagating against the layer flow. Comparison of the records in Figure 19 shows that the peak radiant energy and therefore the flame luminosity is approximately the same for the 5 cfm (multiple peaks) and 17 cfm flow of natural gas, whereas the peak duration and therefore the flame length is longer for the higher flow rate. This indicates that the initial flammable volume was the same for both flow rates but a greater amount of combustible existed at any location in the gallery with the higher flow rate.

### Burning Pools

Spillage and subsequent ignition of a liquid pool of fuel in an aerospace vehicle poses three hazards: (1) the flame quickly consumes oxygen needed to sustain life, (2) toxic products are produced which may be difficult to remove and (3) heat and pressure developed by the fire can cause serious damage. Since an aerospace vehicle may contain an atmosphere whose oxygen content may vary from 20 volume percent at a total pressure of one atmosphere to 100 volume percent at a total pressure of 5 psia, a wide range of burning states would be possible, from a slow deflagration to a detonation. The experiments conducted to date have been concerned primarily with atmospheres containing 21 volume percent oxygen. Further, one is interested in knowing if such combustion processes could be extinguished by venting to the low pressure environment. Therefore, venting experiments have been conducted on pool fires of gasoline, JP-6 and unsymmetrical dimethylhydrazine (UDMH) in air atmospheres. Preliminary studies showed that 1-inch burning pools of JP-6 and UDMH at atmospheric pressure could not sustain combustion if the oxygen concentration of the air-nitrogen atmospheres were less than 17 and 14 volume percent, respectively; a similar study with a burning candle gave a limiting oxygen concentration of 18 volume percent. Since the human body can function at oxygen concentrations as low as 14 volume percent for appreciable lengths of time without endangering life (ref. 12), small liquid fires could be safely extinguished if the oxygen concentration of the atmosphere were lowered with nitrogen below the limiting values noted.

### Low rate of pressure change. -

The initial experiments were conducted with a candle burning in a 12-foot diameter sphere to determine the effect of reduced pressure on the flame shape and appearance. Figure 21 shows a sequence of photographs taken during the course of one experiment as the pressure in the sphere was gradually reduced. The original photographs show that the initially yellow

candle flame begins to acquire a blue base as the pressure drops. The extent of this blue region grows steadily with decreasing pressures until finally just prior to extinguishment the flame is entirely blue. This increasing blue region in the flame is probably attributable to a shift in the combustion reaction toward leaner fuel-air mixtures. Further, the photographs show that the flame lifts up away from the candle top as the pressure falls.

The next series of experiments was conducted in an enclosed apparatus in which the air pressure was permitted to fall gradually while continually maintaining an uncontaminated atmosphere. Liquid regression rates were measured in 1-inch diameter trays\* for JP-6 and UDMH. The results obtained with these fuels are given in Figure 22. This figure shows that with JP-6 the measured regression rates remained essentially independent of pressure down to approximately 0.2 psia. At this pressure the liquid boiled vigorously and a slight increase in rate was noted; with a further decrease in the pressure the flame was extinguished. The liquid regression rate of a burning pool of liquid UDMH under similar conditions showed a very pronounced increase in the liquid regression rate with decreasing pressure. Further, in both cases, as the pressure dropped, the length of the flame over the burning pools increased by as much as a factor of two. As the extinguishment limit was approached with UDMH, the flames became very wispy in nature and the separation between the flame and the liquid surface increased. Eventually, at the limit, the UDMH flames momentarily engulfed the interior of the apparatus and vigorous boiling was evident.

#### High rate of pressure change. -

Further experiments were conducted to determine if the rate of pressure change influenced the burning characteristics of liquid pools. In these experiments, a 24-inch diameter sphere containing the burning liquid in a 4-inch tray at atmospheric pressure was vented into an evacuated 12-foot diameter sphere at 0.01 psia (Appendix I). The initial rate of pressure fall in the 24-inch sphere was approximately 4 psi/sec; in a typical experiment the pressure fell to 0.02 psia in about 18 sec. Pressure histories were obtained in these tests for pools of burning gasoline and UDMH. Typical pressure records obtained within the 24-inch sphere are given in Figure 23. For comparison, a similar record of the pressure history is shown for venting tests without the burning liquid (a) and also for a homogeneous gas phase explosion of gasoline-vapors in air (c). These records show that with the exception of the initially small increase in pressure due to the burning of the liquid pool (b), the pressure records for the two experiments conducted with and without burning liquids present are similar. A closed circuit TV monitor permitted visual observation of the burning liquids during the course of these experiments. The characteristics of the burning liquid pools in these tests were similar in all respects to those conducted with the lower rates of pressure fall. The flame length increased with

---

\* The liquid regression rate depends on the tray diameter (ref. 13).

decreasing pressure and just prior to extinguishment the flames suddenly appeared to completely fill the interior of the 24-inch sphere; the pressure records show no abnormal behavior prior to extinguishment. The only difference that might be noted between these experiments and those conducted under low rates of pressure fall is that the pressure at which the flame extinguished was approximately 0.1 psia as compared to 0.5 psia in the previous experiments with the smaller tray.

#### Autoignition in Accelerated Fields

Prior to designing specific experiments to be conducted under zero gravity conditions in the KC-135 aircraft, preliminary experiments were conducted to determine the type and magnitude of the effects to be expected. Since zero gravity conditions are not readily obtained in the laboratory, experiments of this nature were not attempted. However, if gravitational (acceleration) fields affect the autoignition of gaseous systems, then such effects will be observable under accelerated field conditions as well, that is, for acceleration fields in excess of that associated with the earth's gravitational field. Accordingly, autoignition studies of fuel vapor-air mixtures were conducted in spherical heated vessels subjected to radial acceleration fields of 1 g and 10 g magnitude. A complete description of the apparatus is given in Appendix V; the fuel chosen for this study was n-decane, since it has a relatively low autoignition temperature (405° F) and readily measurable time delays (the order of seconds). Approximately 25 experiments were conducted at about 417° F for both the 1 g and 10 g conditions. An average time delay of 12.5 seconds was obtained at 1 g and 1.5 seconds at 10 g. Figure 24 shows a bar graph of the spread of 0.9 of the experimental points for these two test conditions; the remaining points fell outside the horizontal bars. Although these data are preliminary in nature, they do indicate a possible dependence of the autoignition on the acceleration field strength. Further work is required to verify these findings.

## SUMMARY AND CONCLUSIONS

Pressure records obtained to date for vented hydrogen-air mixtures explosions show two pressure peaks. The first peak appears to be dependent on the rupturing pressure and vent diaphragm inertia and the second larger peak on the vent opening size.

Flames propagating through quiescent heterogeneous combustible-air mixtures exhibit burning velocities at any point which appear to depend only on the composition of the gas mixture at that point and are not dependent on the previous history of the flame. Further, these velocities are equal to the velocities associated with homogeneous mixtures of corresponding concentrations.

Flammable gas mixture zones resulting from the molecular diffusion of a combustible into air exhibiting large concentration gradients cannot, in general be predicted a priori from diffusion theory. Although the position of flame extinguishment at the lean limit is in general predictable from diffusion theory, the position of extinguishment at the rich limit is not predictable.

Richardson's number appears to be a valid criterion for mixing processes in flowing stratified systems. Flames associated with flowing stratified systems have speeds considerably greater than those associated with corresponding homogeneous mixtures.

Venting a liquid pool fire to a low pressure environment tends to increase the liquid regression rate and the flame size. The more volatile the liquid the more pronounced the effect. Since a fire in an aerospace vehicle compartment consumes oxygen, generates toxic products and develops heat and pressure, it should be emphasized that to the extent practicable all flammable fluid storage tanks and lines should be located and routed so as to preclude any possibility of leakage into crew compartments.

Gravitational fields appear to influence the autoignition characteristics of fuel-air systems.

## PROPOSED INVESTIGATIONS

Explosion venting studies should be continued with both homogeneous and heterogeneous mixtures to determine the effects of vent size, time at which the vent is actuated, and environmental pressures on explosion pressures and vented flames.

Layering studies conducted to date with nonreactive mixtures indicate that the extent of the flammable zones that are formed at an interface can be predicted fairly well by considering molecular diffusion and flow parameters alone. However, the presence of a temperature gradient affects mixing so that reactive systems should give results that differ markedly from those obtained with nonreactive systems. These results should be investigated at atmospheric and reduced pressures to obtain a better understanding of the effects of layering on mixture formation in both nonreactive and reactive systems.

The use of electrical and electronic equipments in flammable mixtures creates a hazard unless the equipments are explosion-proof. This requires design data on the ignition of such mixtures and the transmission of flame through various openings (flanges, screwed fittings, etc.). Such data are currently not available on many of the new fuels of interest. Apparatus currently available can be used to obtain the data needed for the design of realistic acceptance test equipment for use with fuels such as hydrazine, pentaborane and unsymmetrical dimethylhydrazine.

## REFERENCES

1. Van Dolah, Robert W., Zabetakis, Michael G., Burgess, David S., and Scott, George S. Review of Fire and Explosion Hazards of Flight Vehicle Combustibles. ASD Technical Report 61-278, 1961.
2. Scott, George S., Perlee, Henry E., Martindill, George H., and Zabetakis, Michael G. Review of Fire and Explosion Hazards of Flight Vehicle Combustibles. ASD Technical Report 61-278, Supplement 1, 1962.
3. Cabbage, P. A., and Simmonds, W. A. An Investigation of Explosion Reliefs for Industrial Drying Ovens. The Gas Council, Research Communication GC 23 (London), 1955.
4. Cabbage, P. A., and Simmonds, W. A. An Investigation of Explosion Reliefs for Industrial Drying Ovens. The Gas Council, Research Communication GC 43 (London), 1957.
5. Simmonds, W. A., and Cabbage, P. A. The Design of Explosion Reliefs for Industrial Drying Ovens. Proc. of the Symposium on Chemical Process Hazards. Inst. of Chemical Engineers (London), 1960.
6. McCabe, Warren L., and Smith, Julian. Unit Operations of Chemical Engineering. McGraw-Hill Book Co., New York, 1956, p. 928.
7. Curtiss, Charles F., and Hirschfelder, Joseph O. Transport Properties of Multicomponent Gas Mixtures. J. Chem. Phys., v. 17, 1949, pp. 550-5
8. Coward, H. F., and Hartwell, F. J. Studies in the Mechanism of Flame Movement. I. The Uniform Movement of Flame in Mixtures of Methane and Air, in Relation to Tube Diameter. J. Chem. Soc., 1932, pp. 1996-2004.
9. Richardson, L. F. The Supply of Energy from and to Atmospheric Eddies Proc. Roy. Soc. (London), v. A97, 1920, pp. 354-73.
10. Ellison, T. H., and Turner, J. S. Turbulent Entrainment in Stratified Flows. J. Fluid Mech., v. 6, 1959, pp. 423-448.
11. Bakke, F., and Leach, S. J. Methane Roof Layers. Safety in Mines Research Establishment, Research Report No. 195, November 1960.
12. Berger, L. B., and Davenport, S. J. Effects of the Inhalation of Oxygen. BuMines Inf. Circ. 7575, 1950, p. 11.
13. Burgess, D. S., Strauser, A., and Grumer, J. Diffusive Burning of Liquid Fuels in Open Trays. Fire Research Abstracts and Reviews, v. 3, 1961, pp. 177-192.

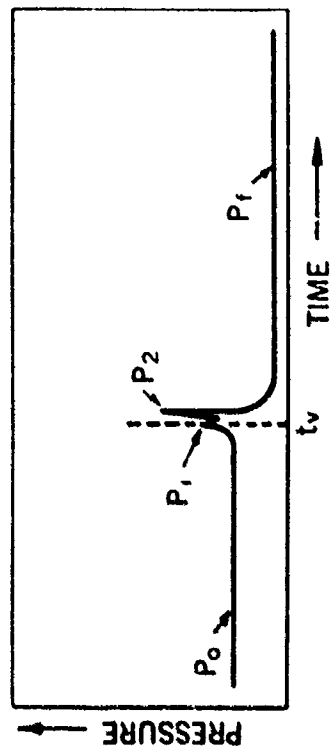


Figure 1. - Pressure trace produced following the ignition of a uniform hydrogen-air mixture in a vented enclosure.

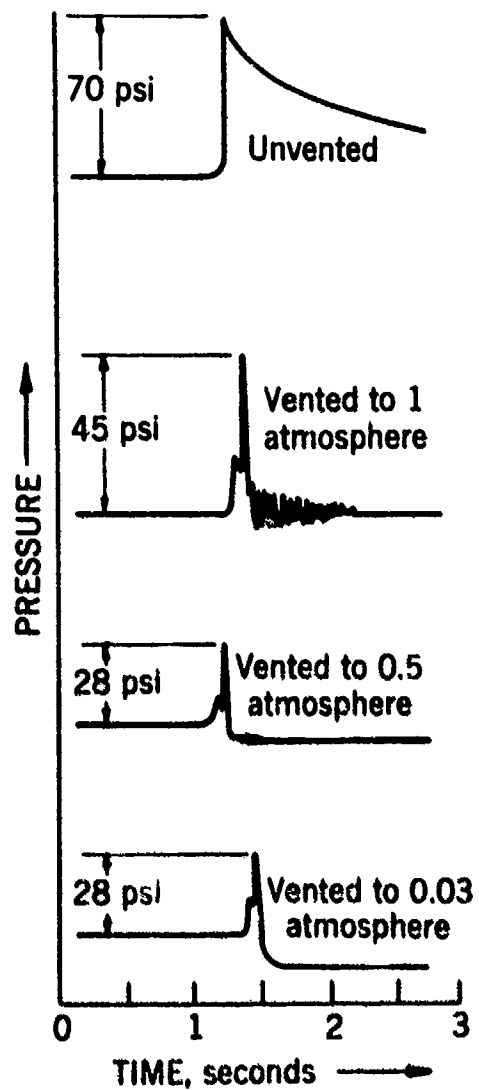


Figure 2. - Pressure traces produced following the ignition of a uniform hydrogen-air mixture containing 13 volume percent hydrogen for various external vent pressures.



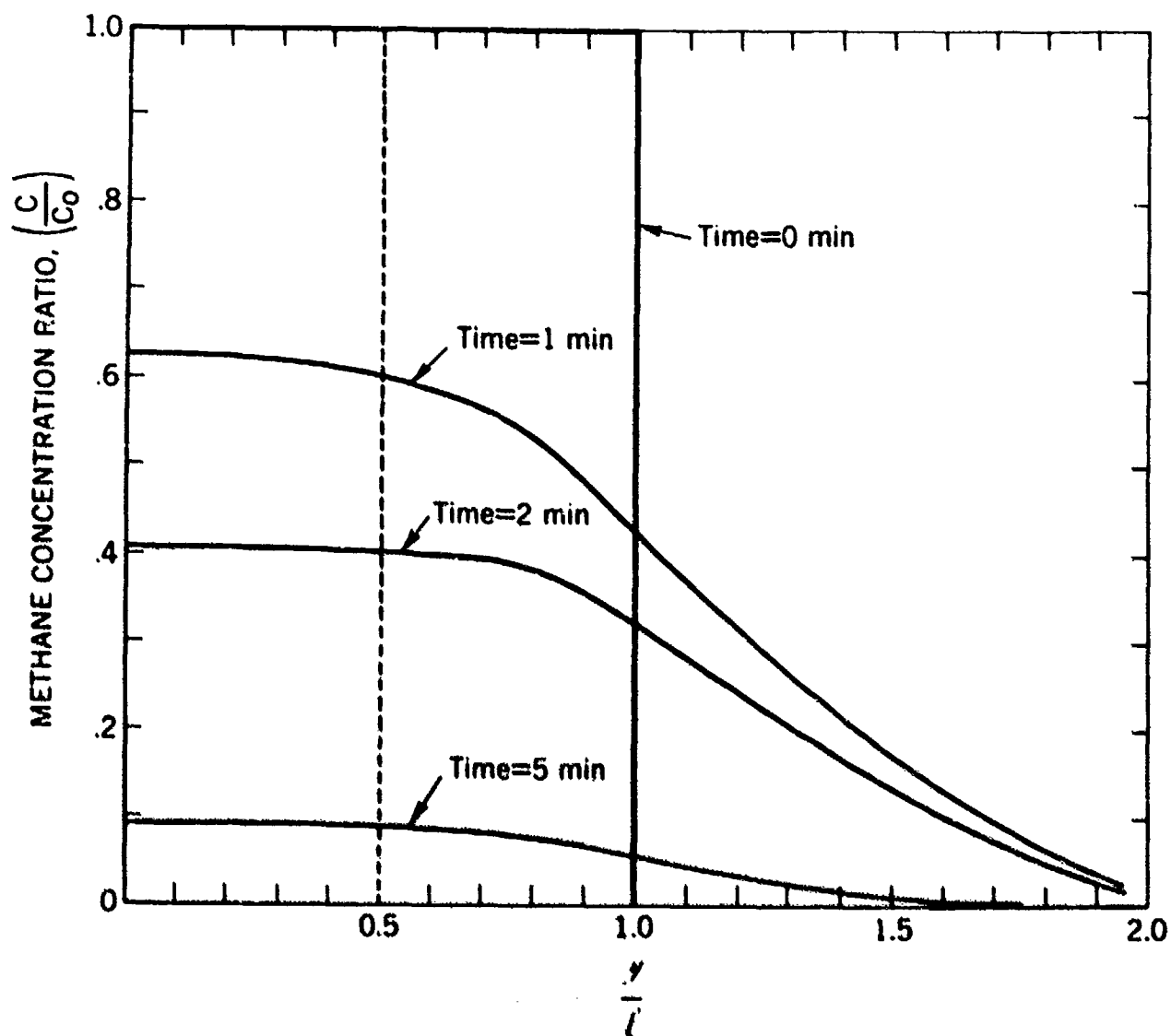


Figure 3. - Concentration profiles of methane diffusing downward into air for a homogeneous methane-air mixture with an initial concentration  $C_0$  and an initial depth  $l$ .

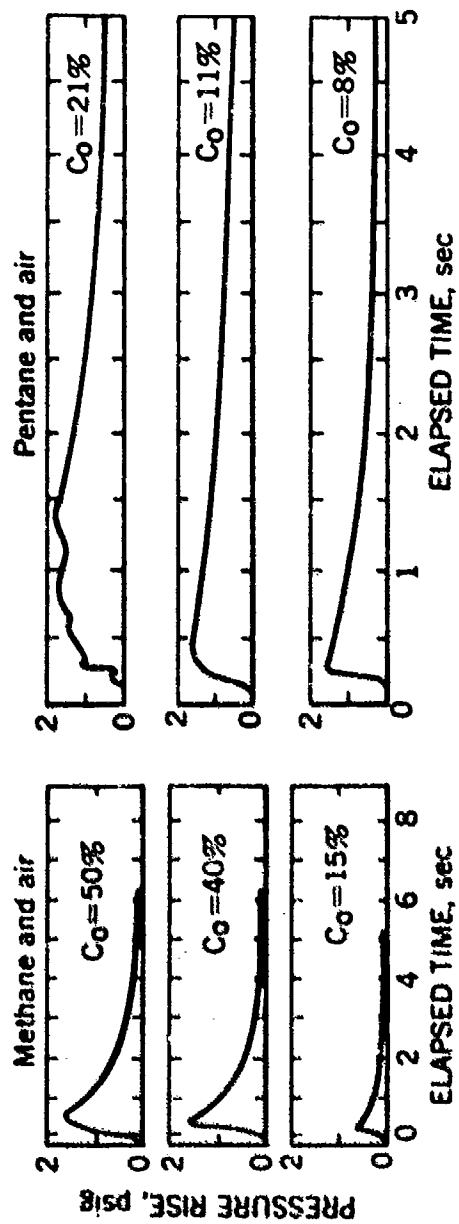


Figure 4. - Pressure records obtained during the combustion of stratified layers of methane-air and pentane-air mixtures in air after a diffusion time of 2 minutes.

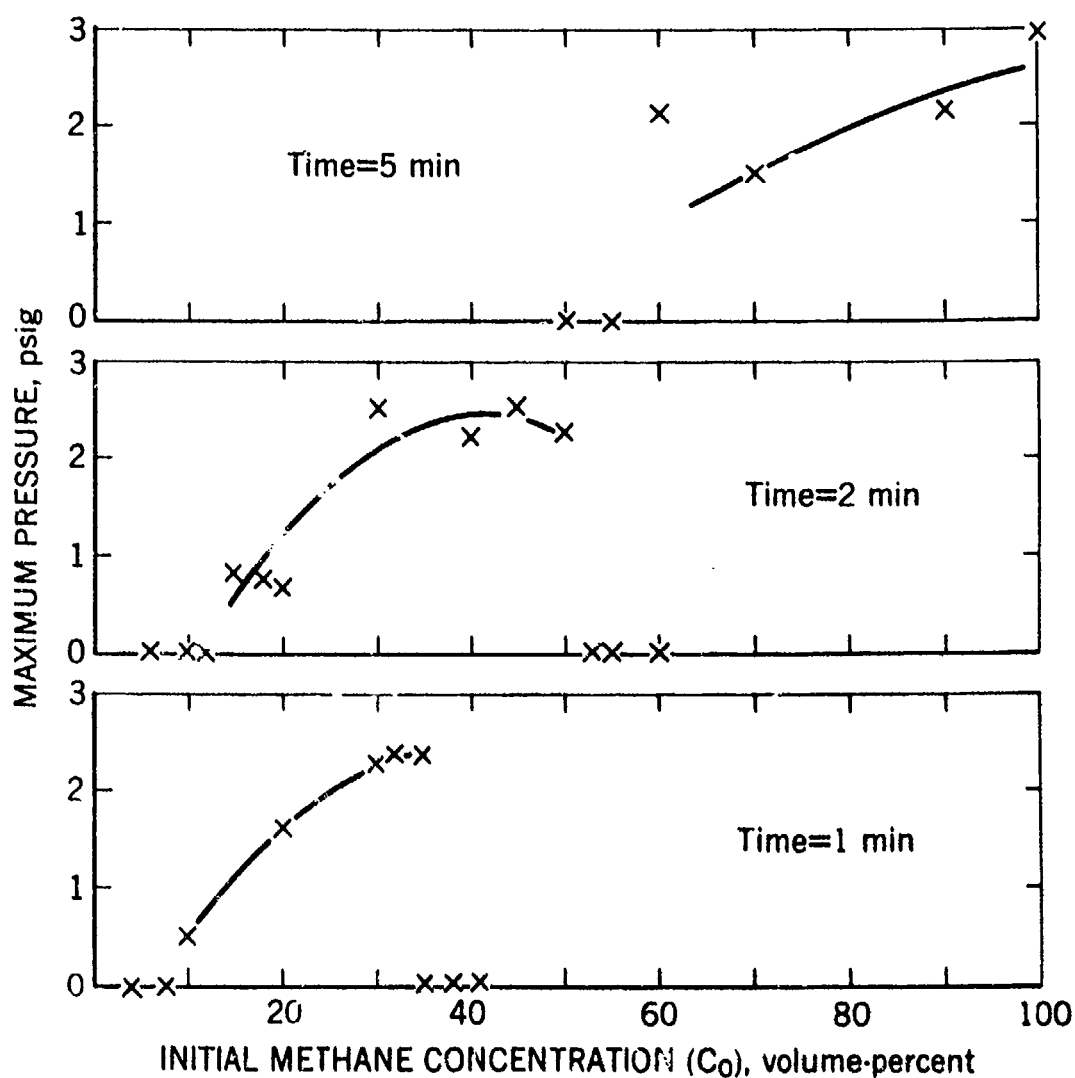


Figure 5. - Maximum pressures developed during the combustion of stratified layers of methane-air mixtures in air for various diffusion times, and initial methane concentrations,  $C_0$

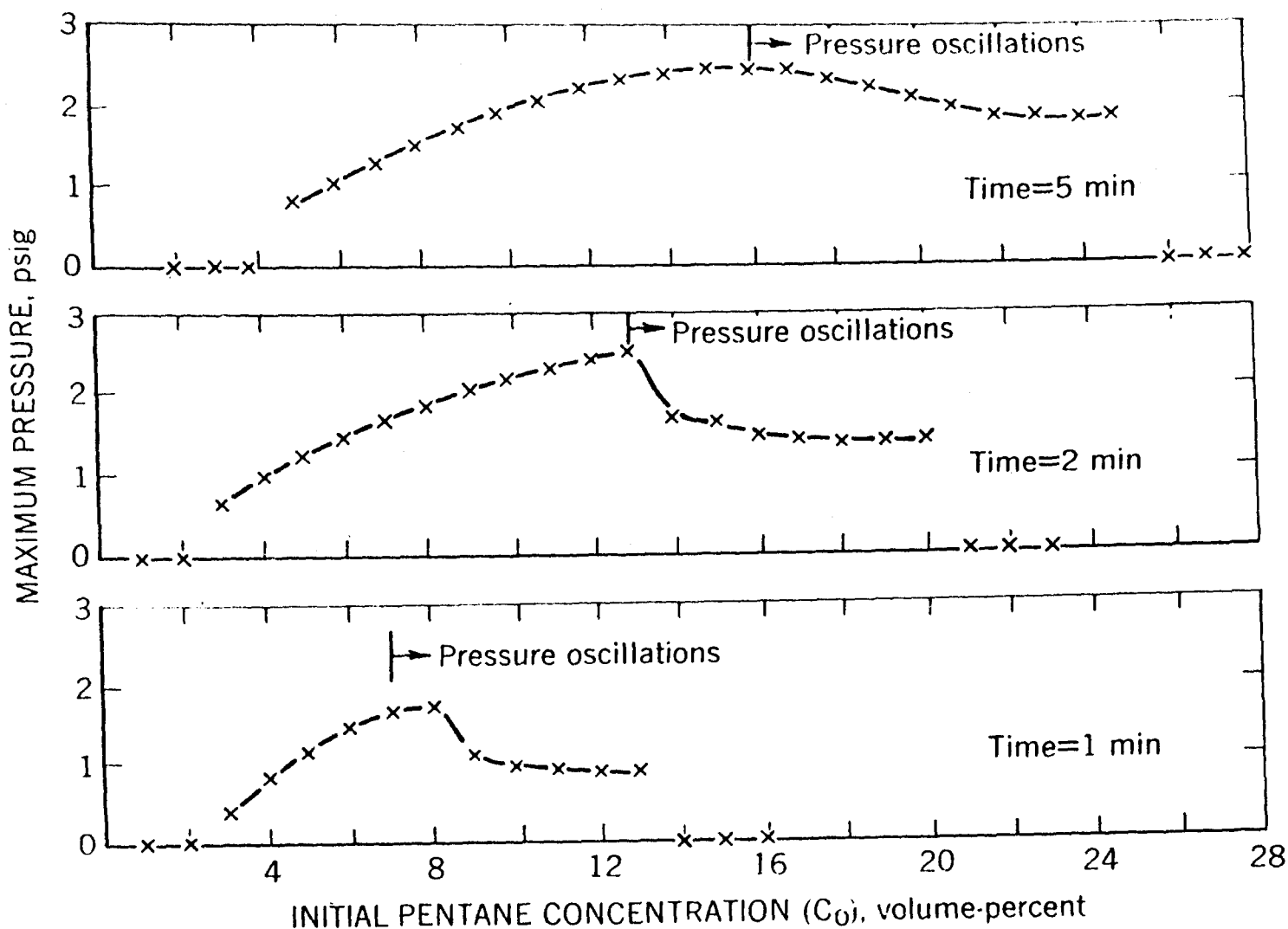


Figure 6. - Maximum pressures developed during the combustion of stratified layers of pentane-air mixtures in air for various diffusion times, and initial pentane concentrations,  $C_0$ .

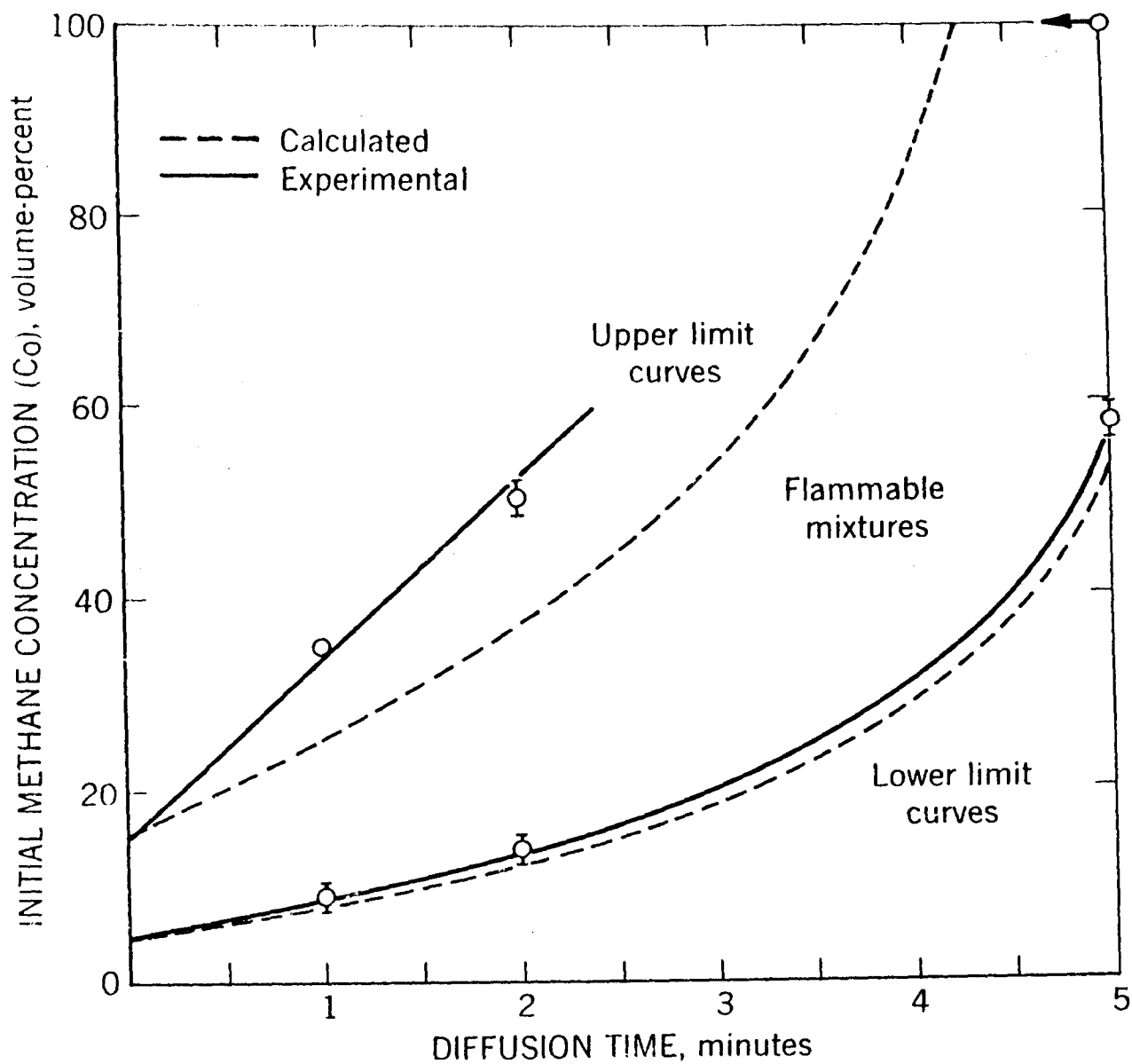


Figure 7. - Range of flammable mixture compositions formed from the diffusion of methane into air at 75° F.

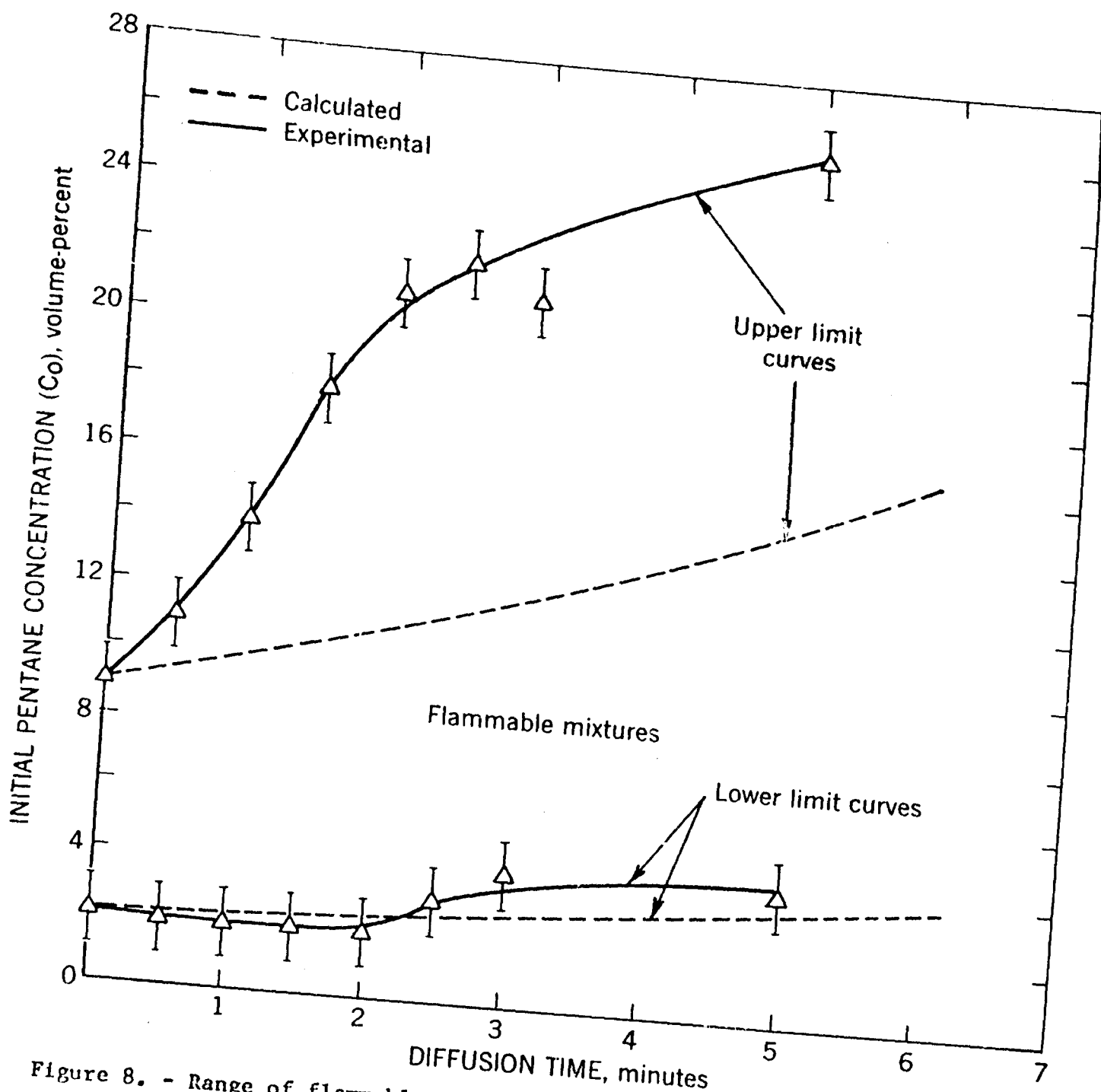


Figure 8. - Range of flammable mixture compositions formed from the diffusion of pentane into air at 75° F.

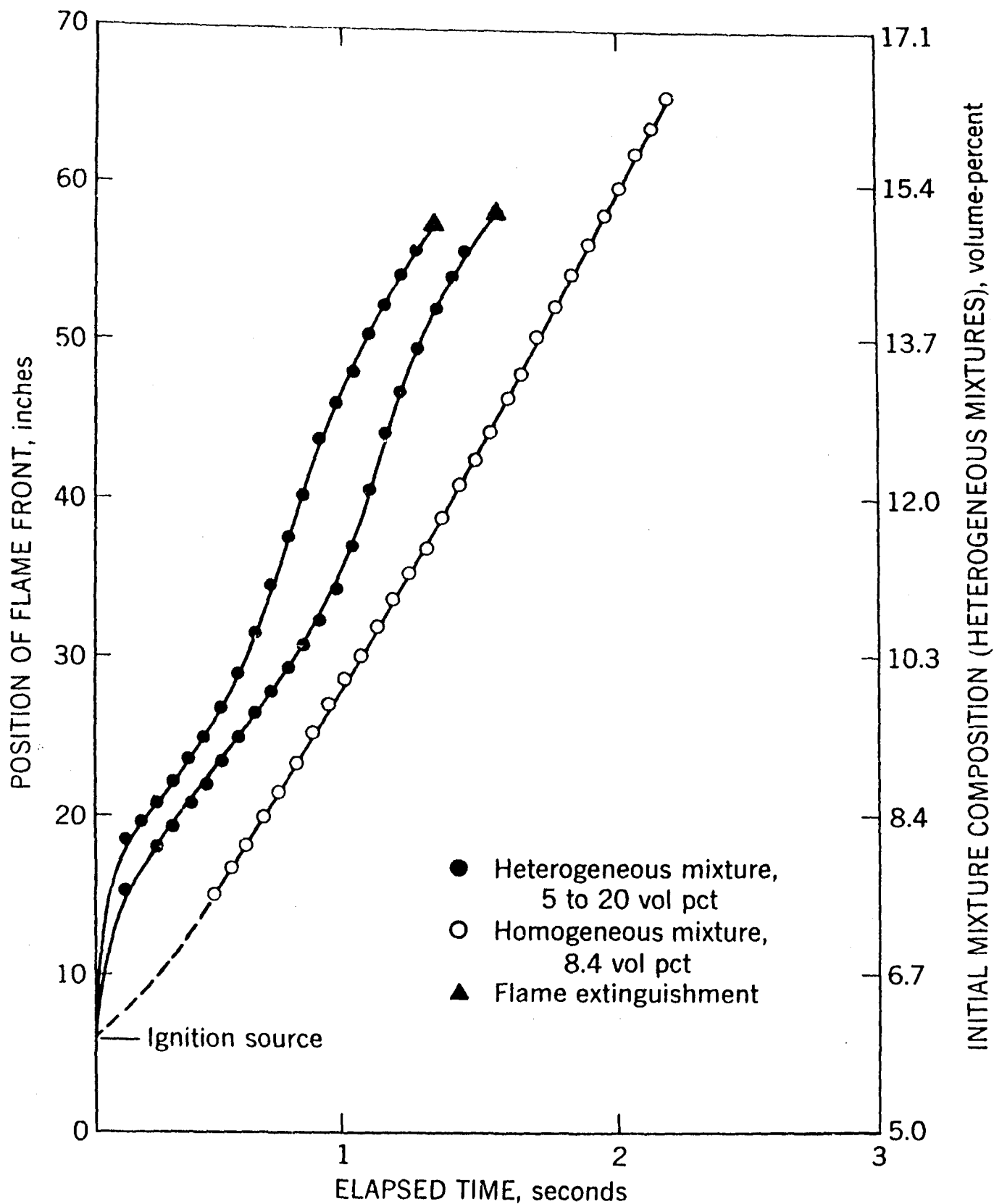


Figure 9. - Position of flame front along a vertical 4-inch tube following ignition of two heterogeneous and one homogeneous methane-air mixtures at atmospheric pressure and 75° F.

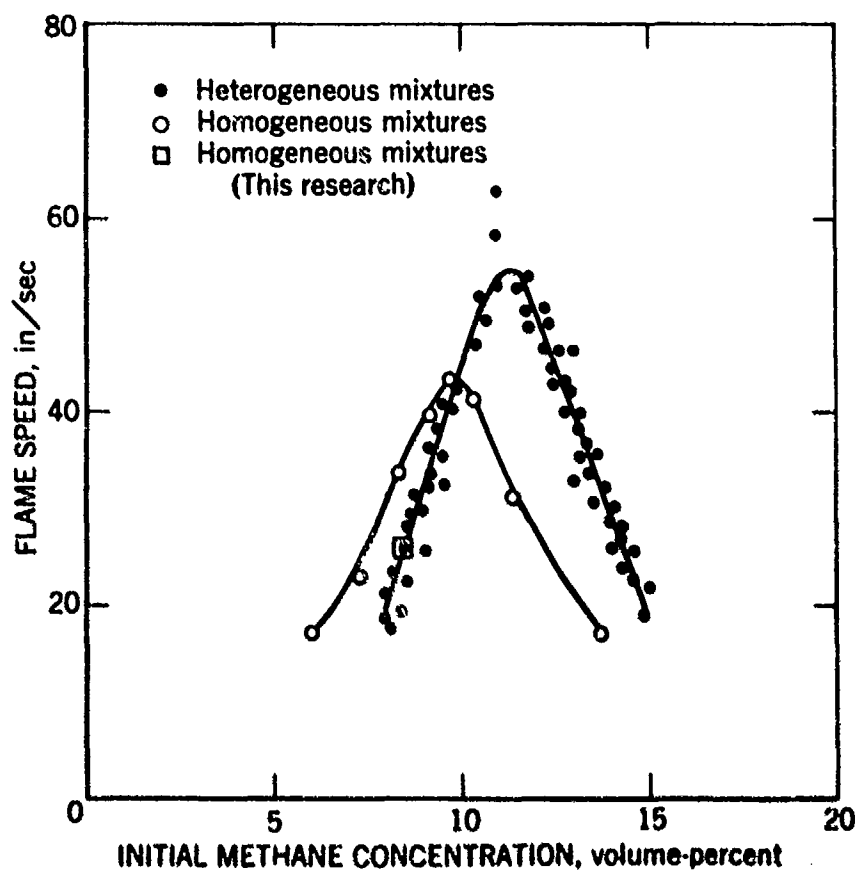


Figure 10. - Flame speeds through homogeneous and heterogeneous methane-air mixtures in 4-inch cylindrical tubes at atmospheric pressure and ambient temperature.



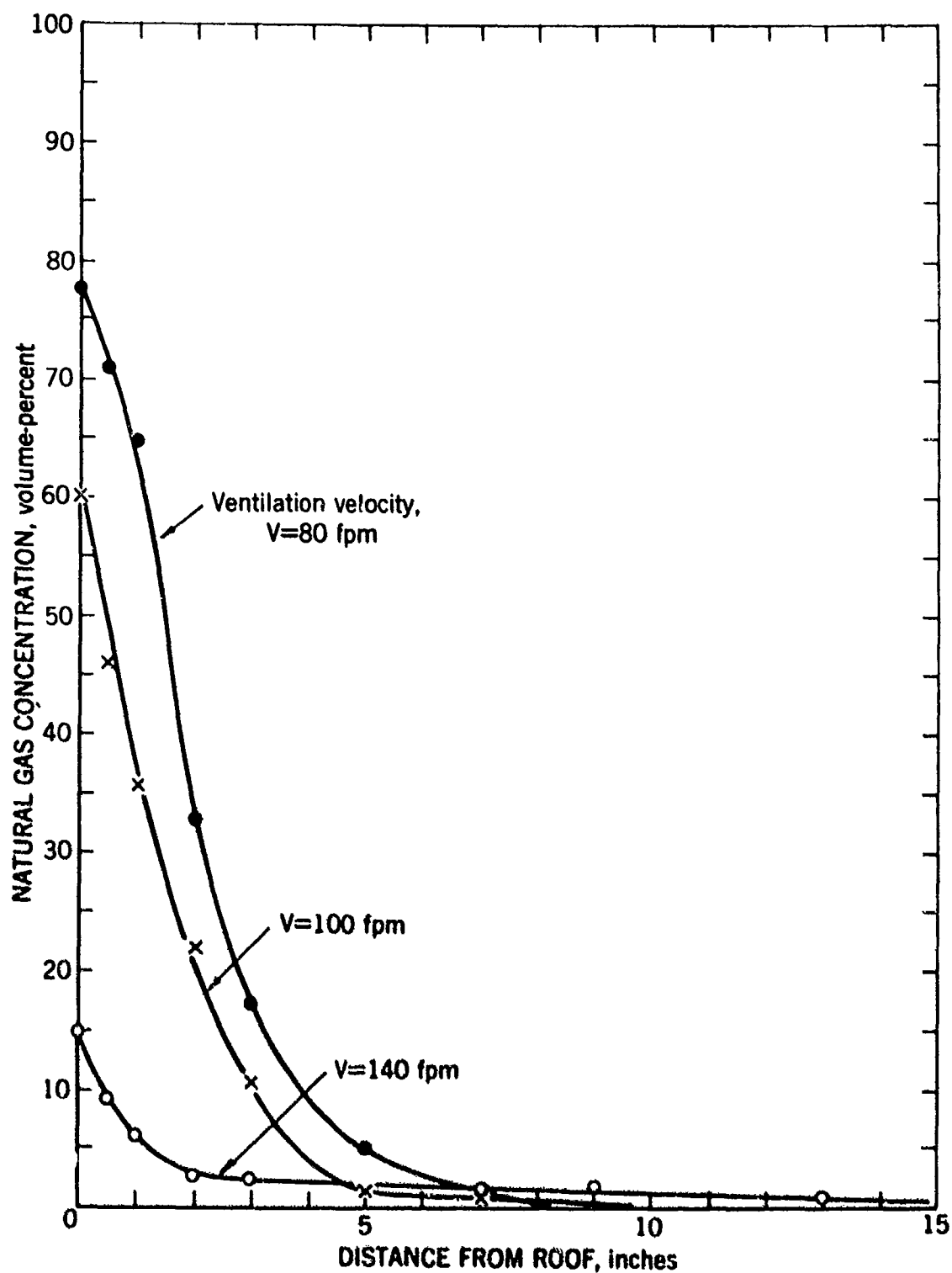


Figure 11. - Concentration of natural gas as a function of distance from the gallery roof, 6-2/3 feet downstream from the gas inlet for a natural gas inlet flow of 5 ft<sup>3</sup>/min and ventilating velocities of 80, 100 and 140 ft/min.

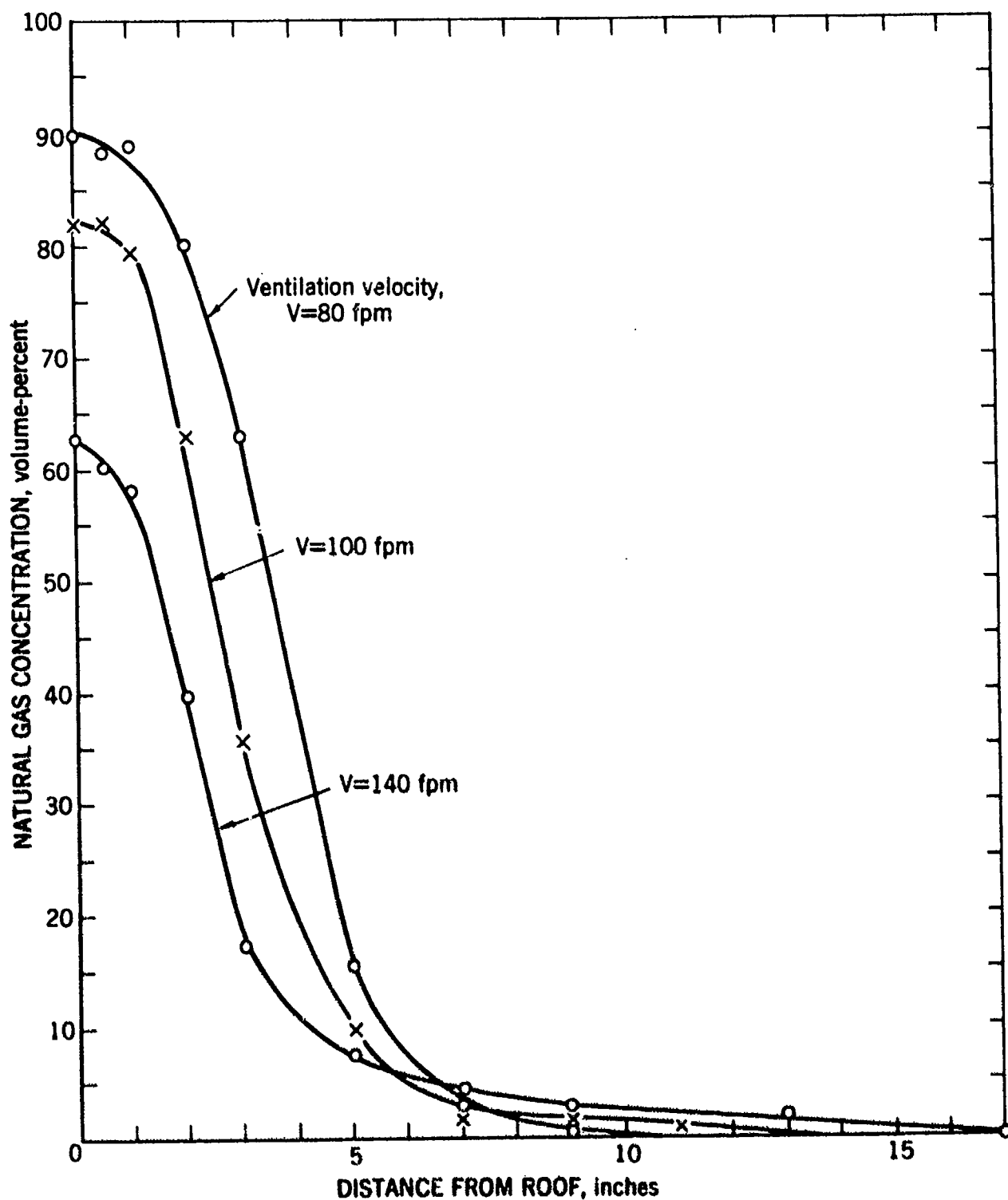


Figure 12. - Concentration of natural gas as a function of distance from the gallery roof, 6-2/3 feet downstream from the gas inlet for a natural gas inlet flow of 17 ft<sup>3</sup>/min and ventilating velocities of 80, 100 and 140 ft/min.

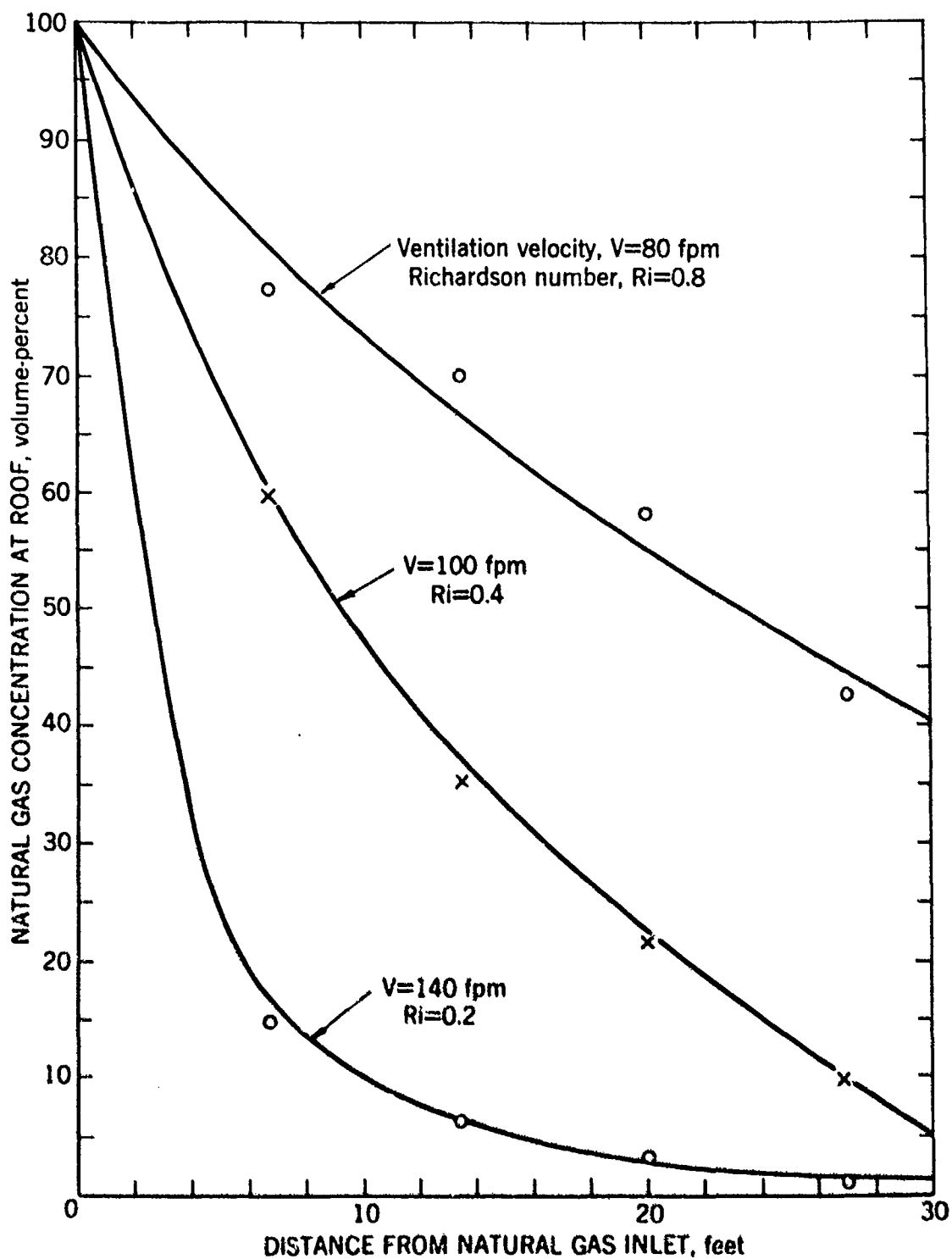


Figure 13. - Concentration of natural gas at the gallery roof as a function of distance from the natural gas inlet (diffuser outlet) for natural gas flow of 5 ft<sup>3</sup>/min showing the effect of ventilation velocity.

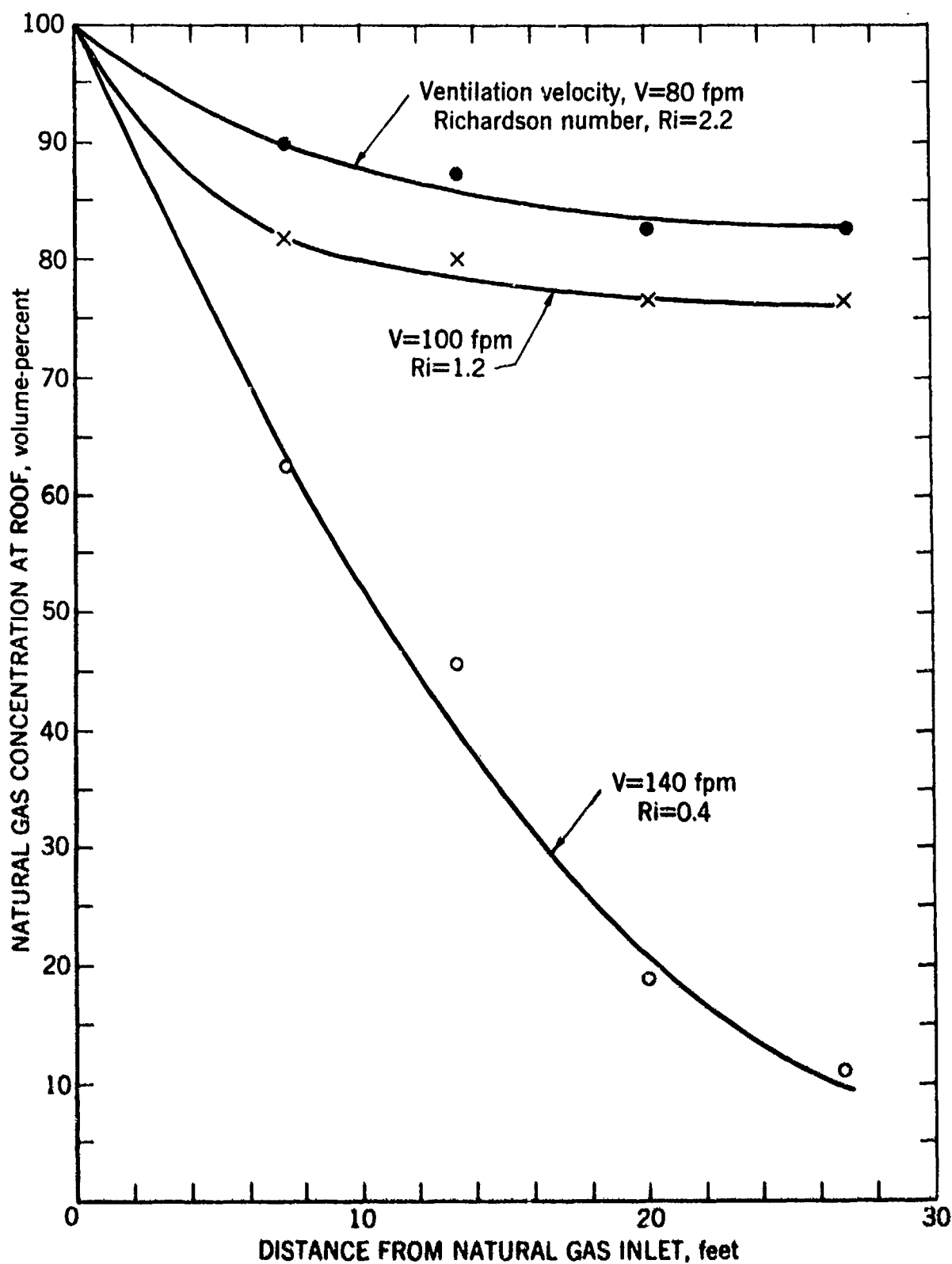


Figure 14. - Concentration of natural gas at the gallery roof as a function of distance from the natural gas inlet (diffuser outlet) for natural gas flow of  $17 \text{ ft}^3/\text{min}$  showing the effect of ventilation velocity.

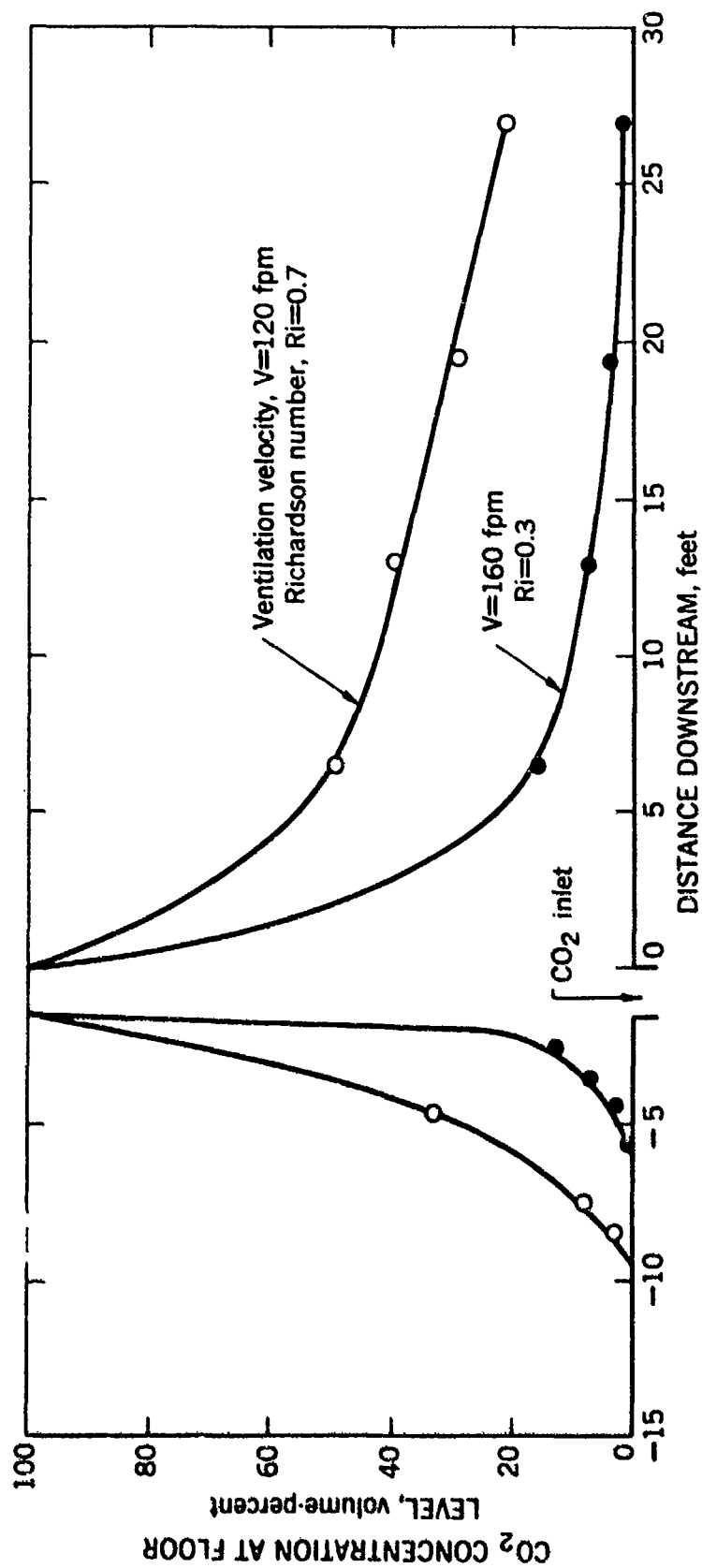


Figure 15. - Concentration of carbon dioxide gas at the gallery floor level as a function of distance from the carbon dioxide inlet showing the effect of ventilating velocity.

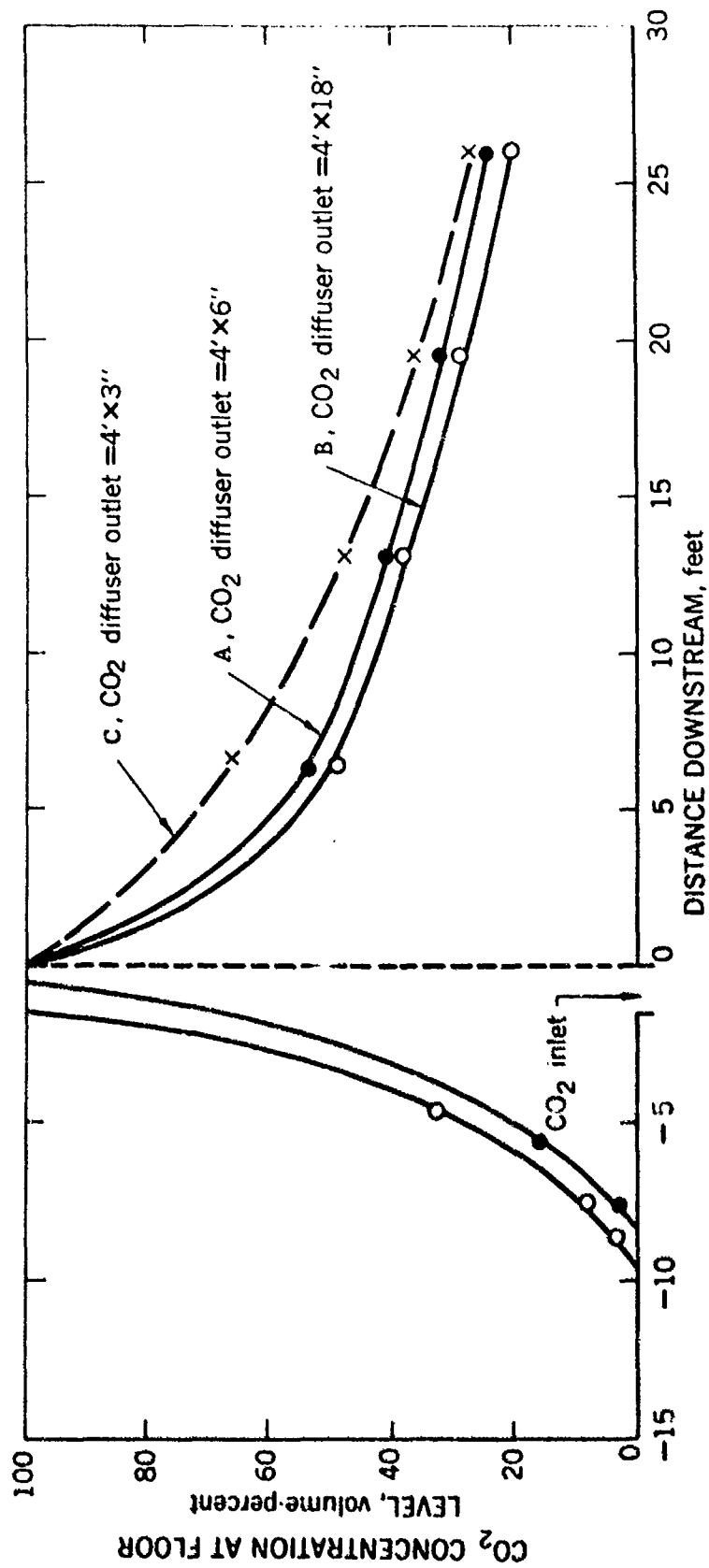


Figure 16. - Concentration of carbon dioxide gas at the gallery floor level as a function of distance from the carbon dioxide inlet showing the effect of variation in CO<sub>2</sub> diffuser outlet design.

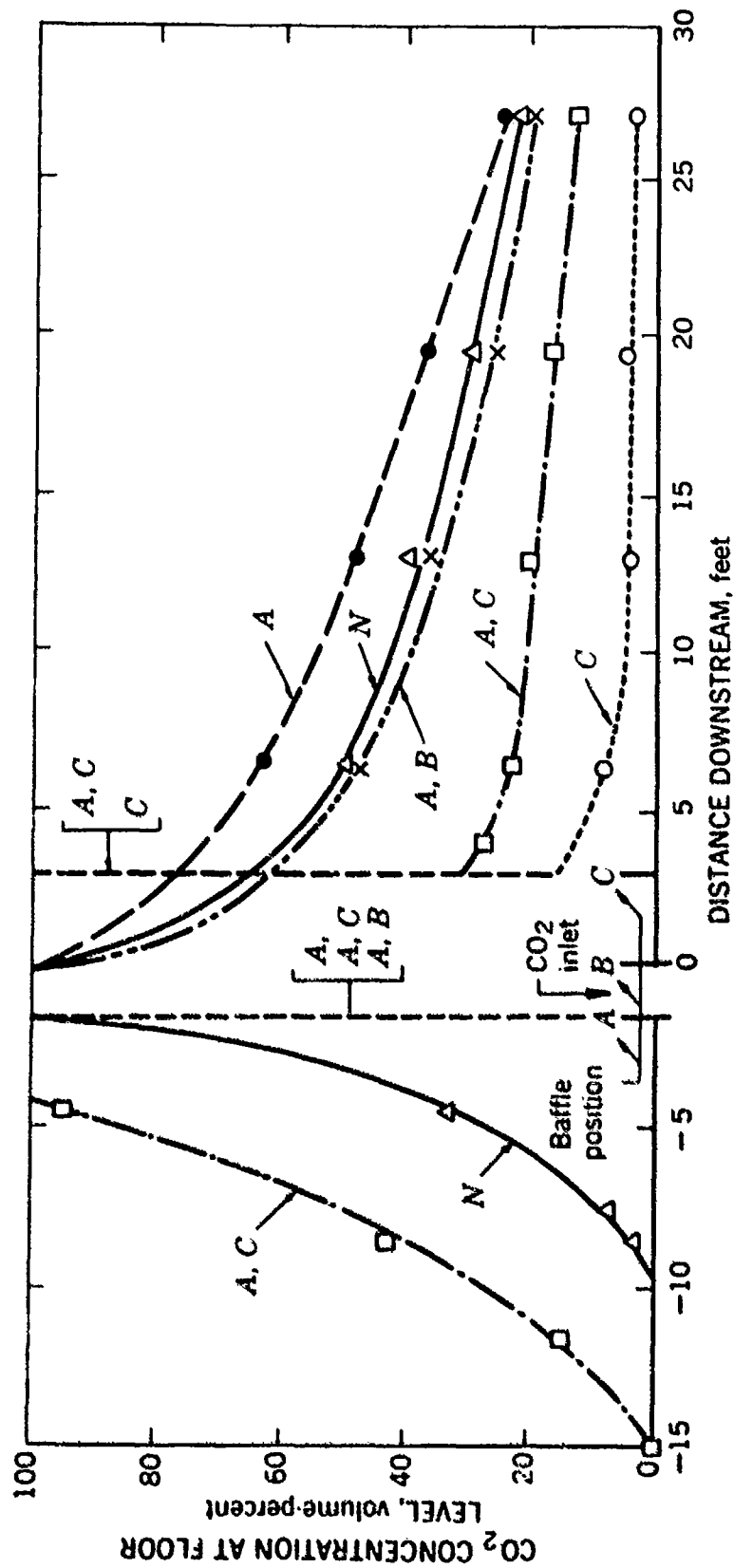
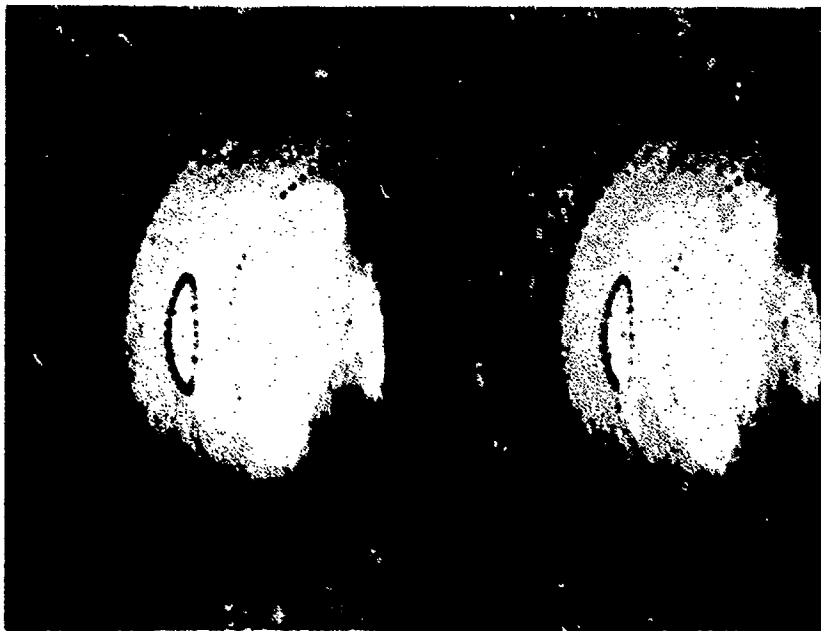
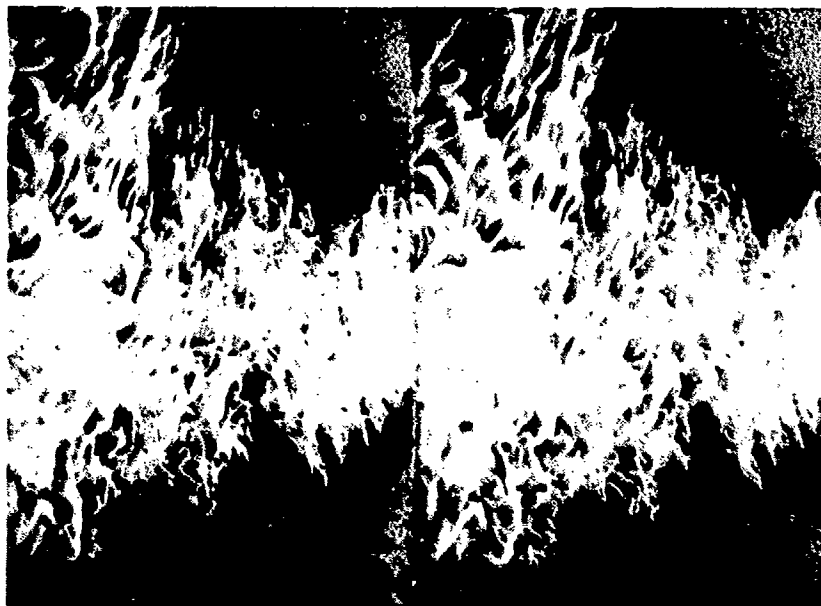


Figure 17. - Concentration of carbon dioxide gas at the gallery floor level as a function of distance from the carbon dioxide inlet, showing the effect of baffle plates placed on the tunnel floor.



Flame traveling downstream  
towards observer



After-burning following the  
initial flame passage

Figure 18. - Two sets of successive frames from motion picture sequence (16 frames/sec) of a flame propagating through a natural gas-air layer in a 6.5 ft-diameter gallery.



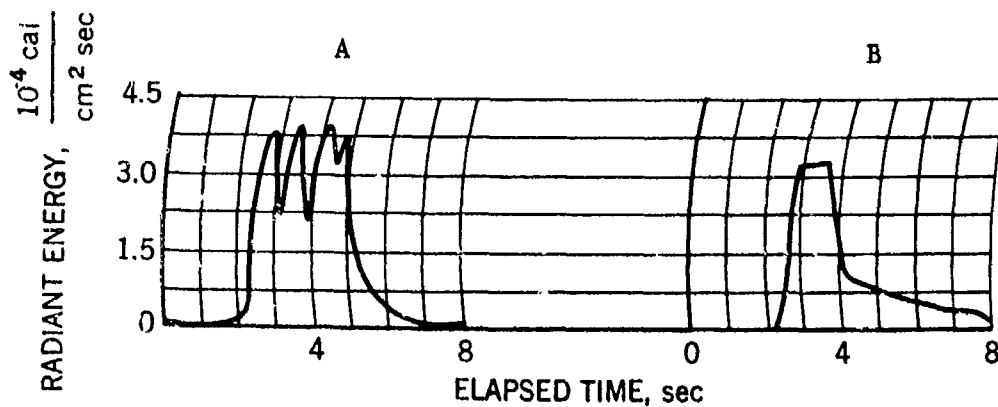


Figure 19. - Radiant energy received on the gallery floor by (A) four photodiodes and (B) one photodiode following passage of a flame through natural gas-air layers along the roof for natural gas flow rates of (A) 5 and (B) 17 cfm.

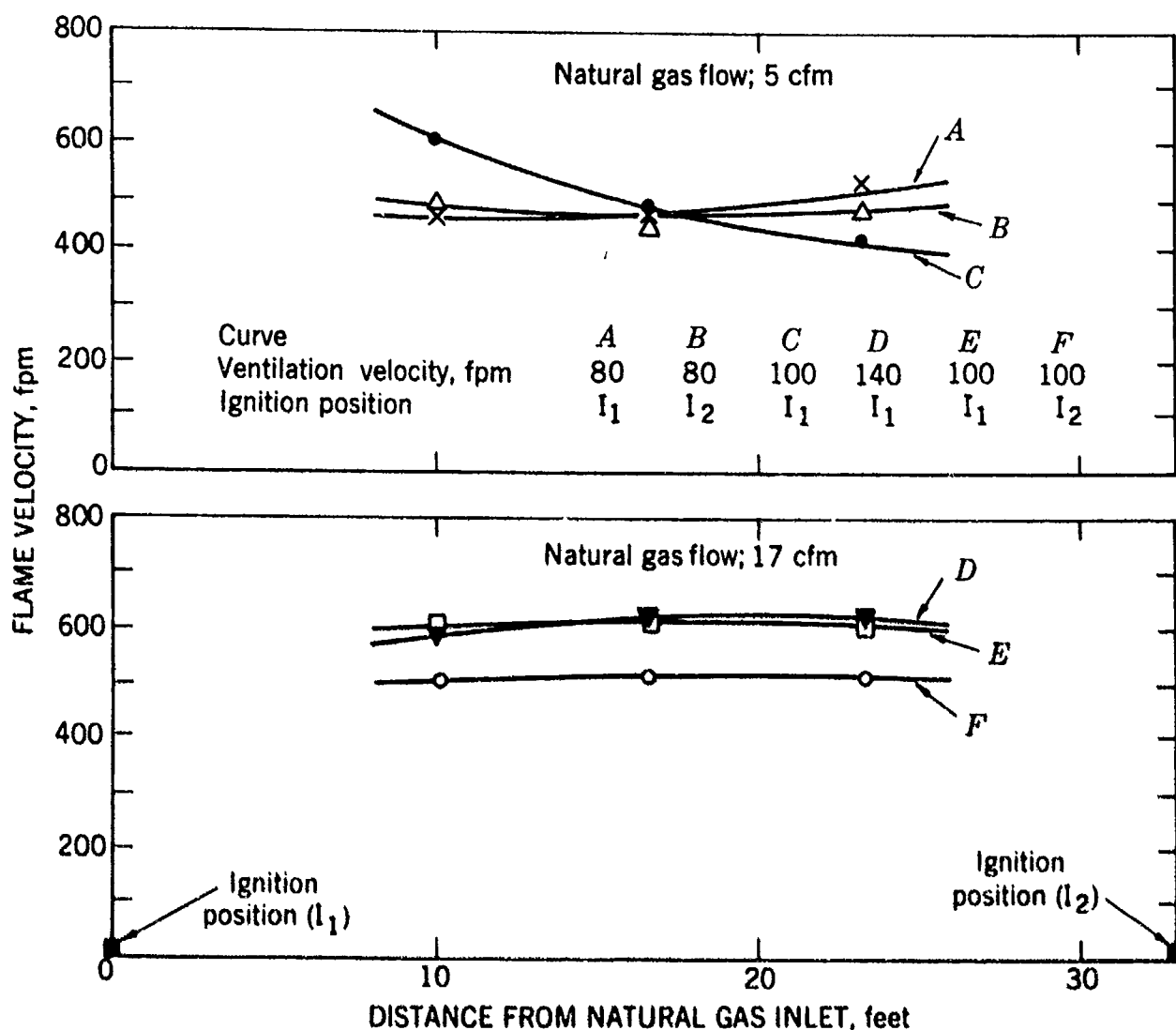


Figure 20. - Effects of natural gas flow rate, ventilation velocity, and location of ignition source on the flame velocity through stratified natural gas-air layers in a 6.5-ft diameter gallery.

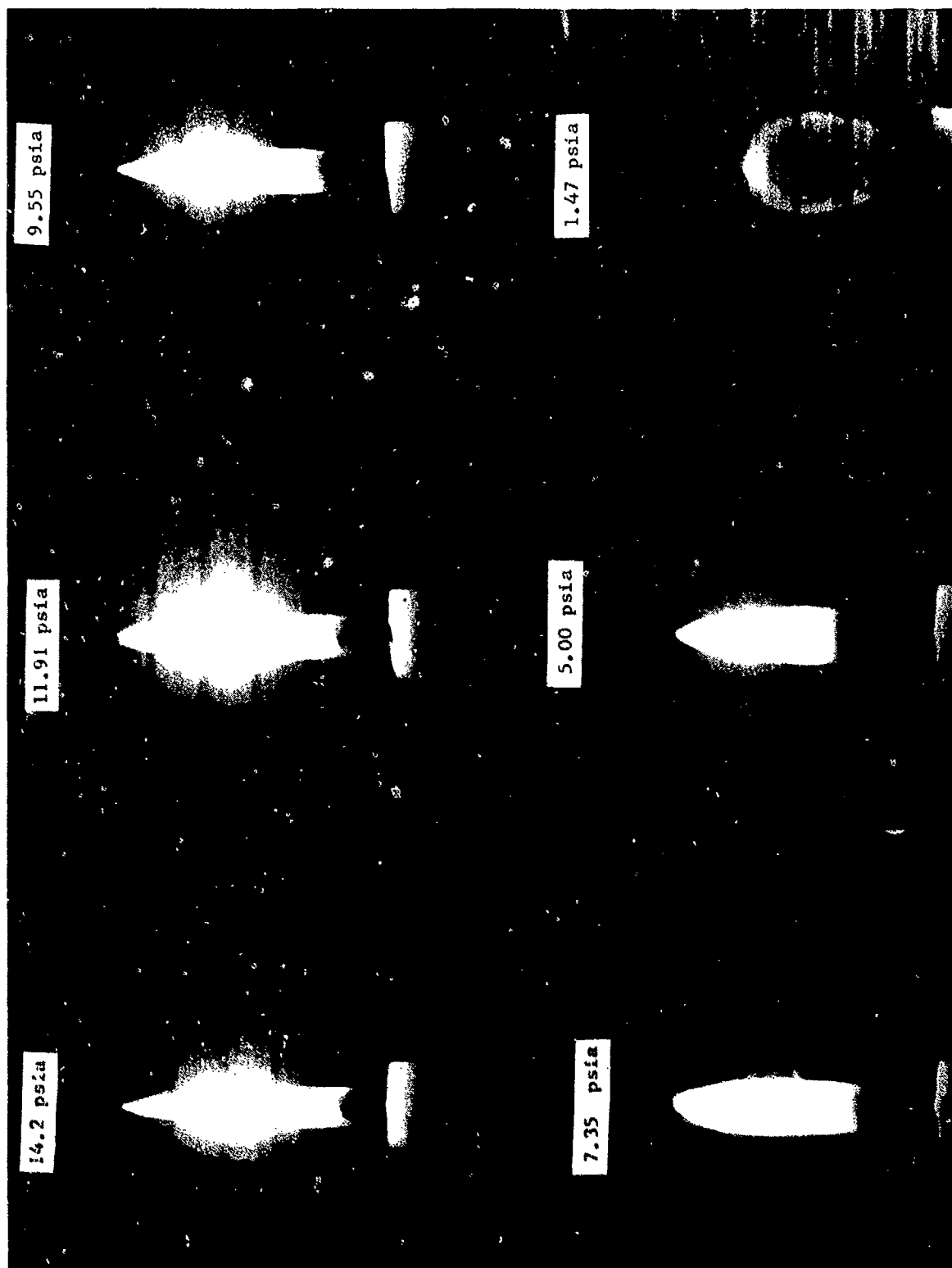


Figure 21. - Photographs of wax candle flame burning in air at various pressures.

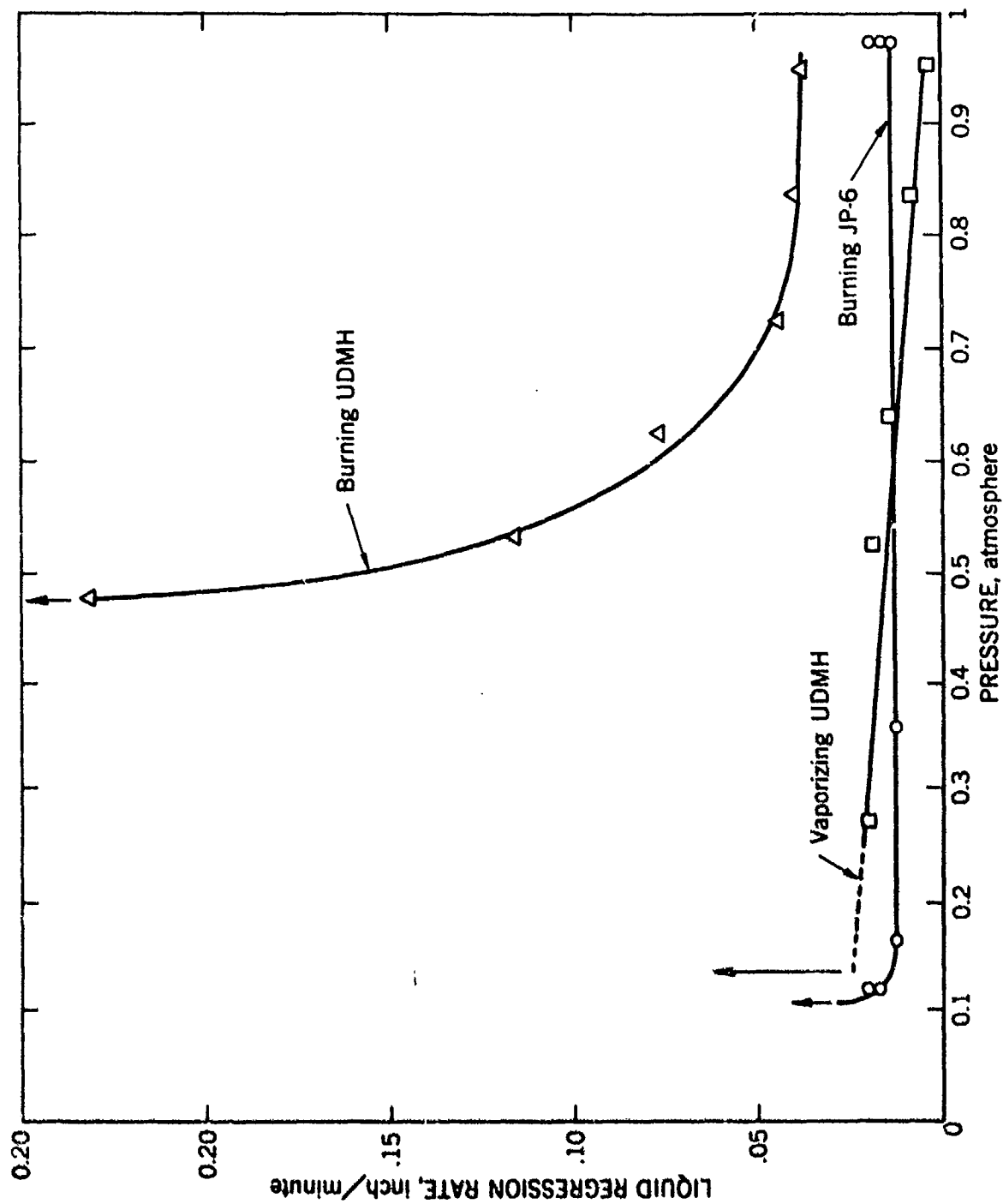


Figure 22. - Liquid regression rate of burning pools of UDMH and JP-6 in one-inch diameter trays as a function of environmental pressure.

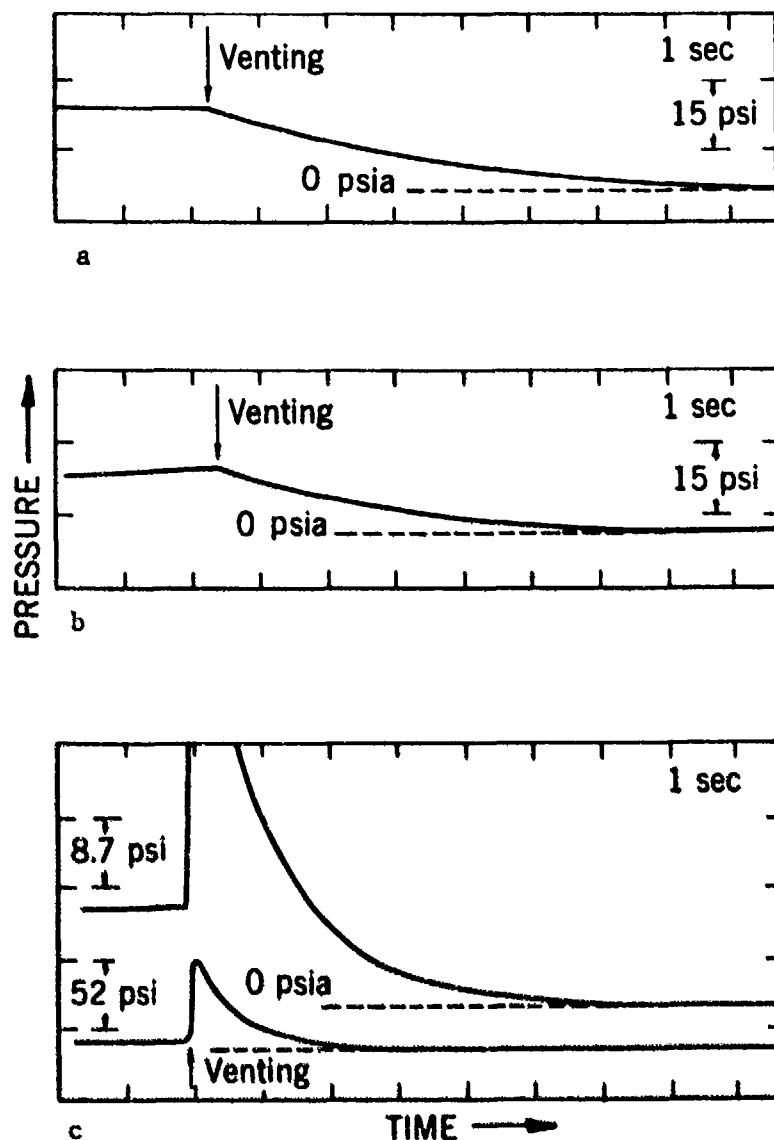


Figure 23. - Pressure histories following (a) venting a 24-inch diameter sphere at 15 psia pressure into a low pressure environment (0.01 psia), (b) venting the same sphere containing a burning pool of liquid UDMH and (c) venting a gas phase explosion of gasoline vapors in air.

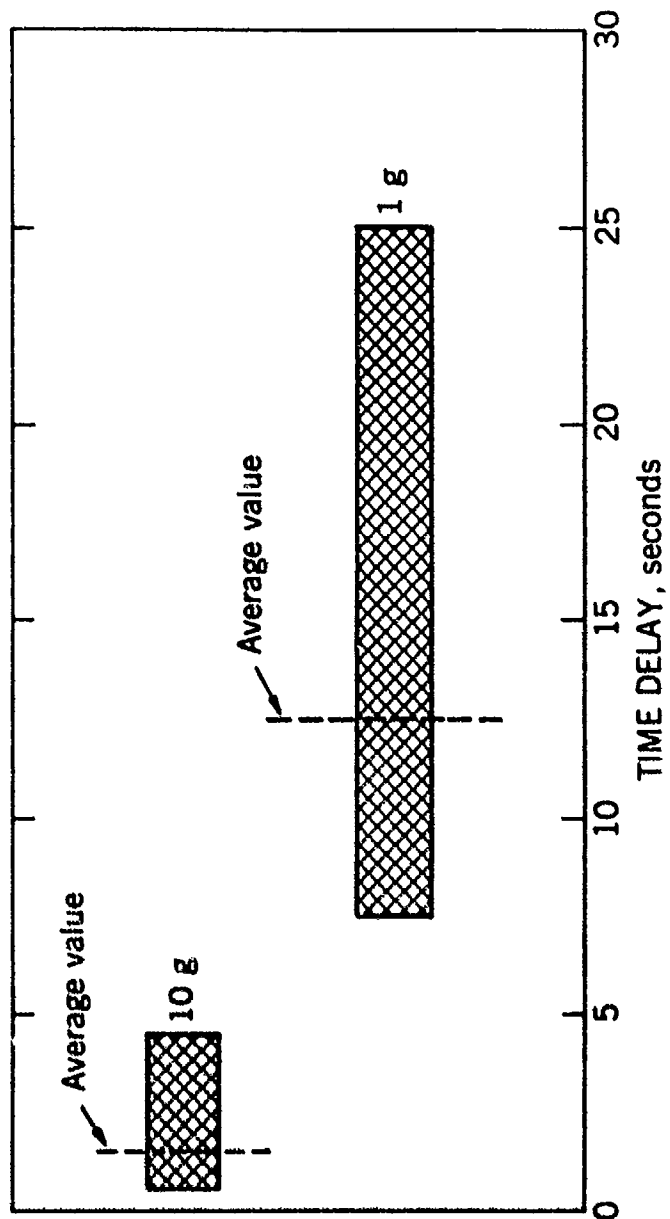


Figure 24. - Autoignition time delays of n-decane in 5-inch diameter stainless steel spherical vessels at 417° F for accelerational fields of 1 g and 10 g.

## APPENDIX I - Low Pressure Chamber

The 12-foot diameter sphere used as a low pressure environmental chamber for venting and pool burning experiments is shown in Figure 25. The sphere is provided with observation and access ports, an access door and a vacuum system; the vacuum pumps are located in an adjacent concrete bunker. A 2-foot diameter sphere (Figure 26) is housed within the low pressure chamber for use in the venting studies. This smaller sphere is equipped with flanged ports for use in the venting experiments. One port (not visible in Figure 26) is equipped with a relief vent and the other with gas inlet tubes, a thermocouple well, spark plug and a Kistler piezo-electric transducer.

To conduct an experiment with a homogeneous mixture, an aluminum foil rupture disk is first mounted in the 4-inch vent port of the 2-foot sphere; conducting silver paint is applied to a shellacked area of the face of the disk and electrical contact to this conducting surface is used to give an indication of the instant of disk failure. A premixed homogeneous mixture prepared in a flow system is used to flush the air from the 2-foot sphere and out to the atmosphere outside the 12-foot sphere. The inlet port is then sealed, the 12-foot sphere evacuated, and ignition effected with a hot wire wrapped with a small quantity of guncotton. The resultant pressure is recorded with a Polaroid camera mounted on a Model 551 Tektronix oscilloscope.

To conduct an experiment with a liquid fuel, a small glass dish (4" dia. x 1") is half-filled with the fuel, the dish is covered with a thin plastic foil to prevent evaporation of the fuel, and then placed in the 2-foot sphere. A small wad of guncotton and an electric match are placed on top of the plastic foil. The electric match is used to ignite the guncotton which in turn burns a hole in the plastic and ignites the fuel. After preparing the small sphere and checking the related equipment, the 12-foot sphere is closed and pumping operations started. Approximately 1-1/2 hours pumping was required to reduce the pressure within the 12-foot sphere to 0.01 psia.

A closed loop television camera located outside the observation port of the 12-foot sphere was used to observe the ignition of the liquid. The liquid was allowed to burn for about 5 seconds before the blow-out diaphragm was ruptured by means of an electric match at the instant,  $t_v$  (Figure 1), noted by the interruption of current through a thin wire on the surface of the diaphragm.

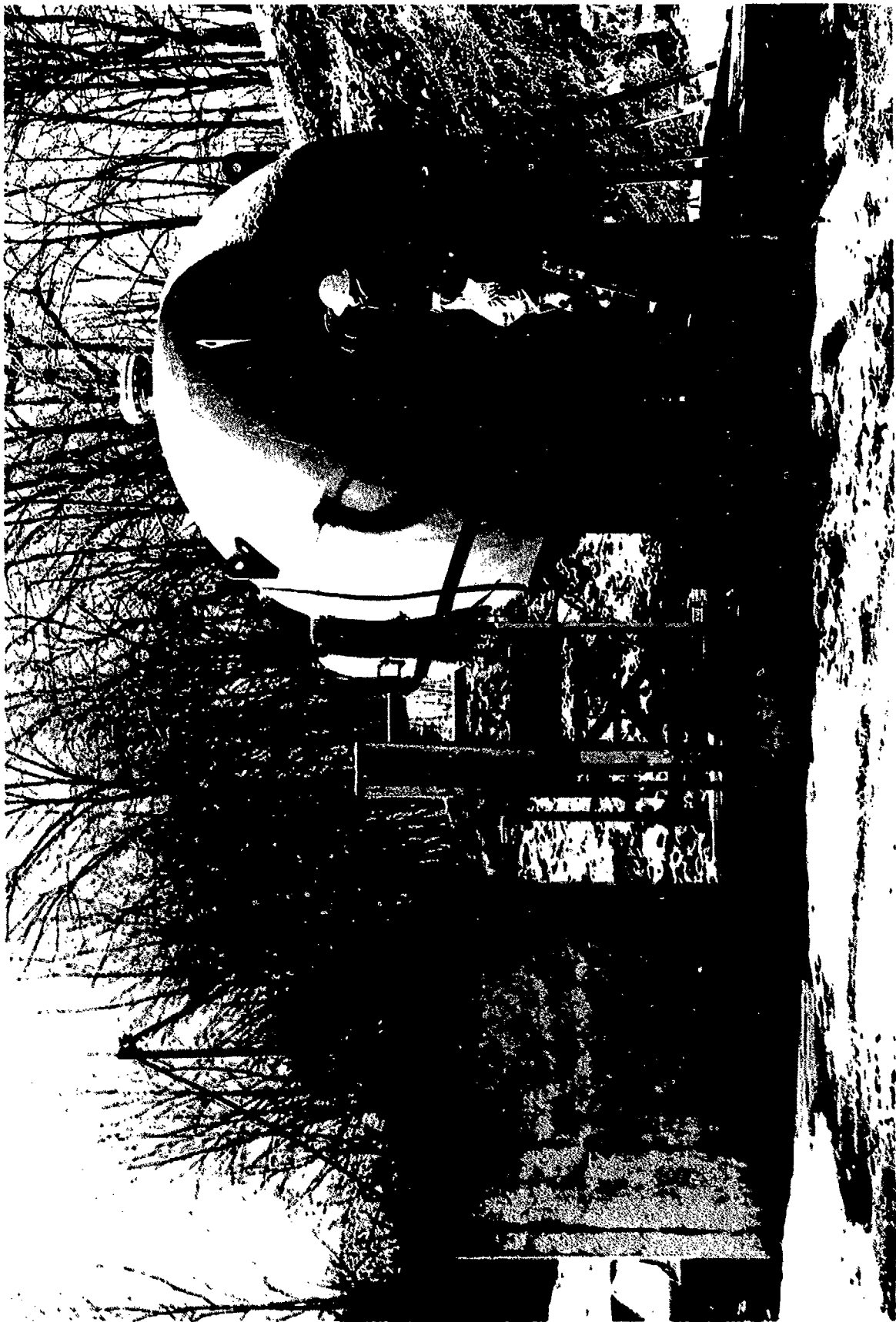


Figure 25. - Twelve-foot low pressure environment sphere.





Figure 26. - Two-foot diameter test sphere.

## APPENDIX II - Quiescent Stratified Mixtures (large concentration gradients)

Figure 27 shows the complete facility used for the quiescent stratification experiments. Flow meters (B) are used in the preparation of the desired initial homogeneous gas mixtures. The sequence timer (F) provides electrical pulses at the appropriate times to start the diffusion process by exposing a homogeneous mixture to the surrounding air atmosphere, trigger the sweep on the oscilloscope and fuse the nickel ignition wire. The stratification sphere (C) provides a gas-tight chamber for the preparation and testing of the heterogeneous mixtures. The pressures developed during combustion are measured with a Fairchild piezo-resistive pressure transducer (D) and recorded with the Polaroid camera-equipped Tektronix oscilloscope, Model 551 (A). The electric clock (E) provides time base for calibration of the sequence timer.

Figure 28 shows the stratification sphere with the top hemisphere removed. A photograph of the upper section with the lower hemisphere removed would show exactly the same mechanical structure. Located between the two hemispheres is a 1-1/2-inch long, 2-inch diameter steel chamber which contains the homogeneous gas mixture to be tested. The spring-loaded sliding vanes (I) provide a gas-tight seal to isolate the homogeneous gas mixture from the surrounding air atmosphere contained in the hemispheres prior to the start of the diffusion process. Both the vane and brass cylinder (G) are provided with Teflon seals. Actuation of the solenoid (H) permits the vane to slide open and simultaneously the brass cylinder to slide in place over the initial homogeneous mixture. The upper hemisphere is used with heavier-than-air gas mixtures and the lower one with lighter-than-air mixtures.

An experiment is conducted by first setting the sequence timer for the desired diffusion time and then purging the chamber with a homogeneous mixture. Upon starting the sequence timer, the solenoid which opens the appropriate vane is actuated to expose the homogeneous mixture to the air-filled brass cylinder. The gas mixture then diffuses into the brass cylinder for a pre-determined time interval (diffusion time), after which the timer triggers the oscilloscope sweep and camera shutter. Ten milliseconds later the nickel ignition wire is fused by a dc current; the pressure record is then removed from the camera and the apparatus is prepared for the next run.



Figure 27. - apparatus used in quiescent stratification experiments.

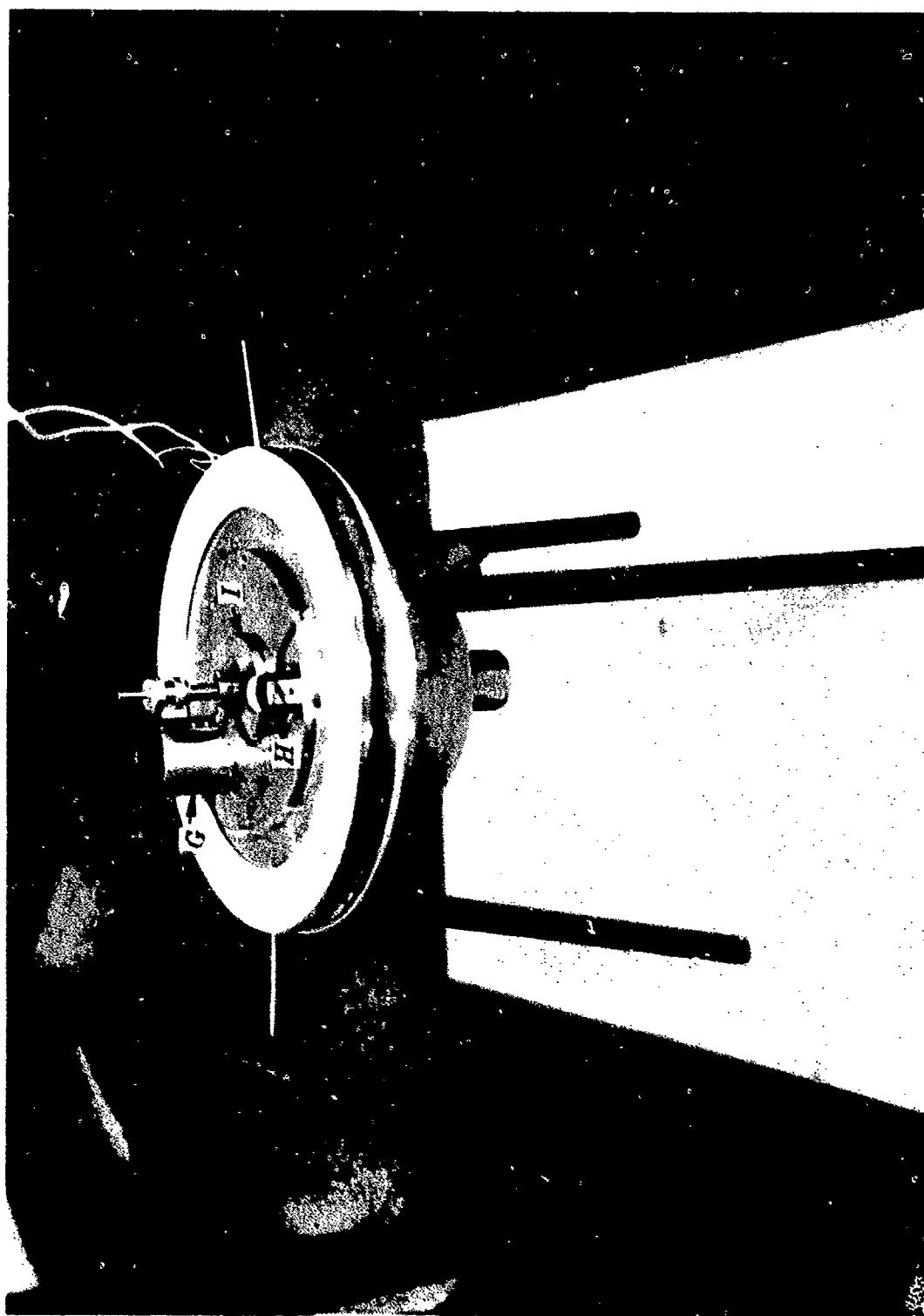


Figure 28. - Lower portion of sphere used in stratification experiments.

### APPENDIX III - Quiescent Stratified Mixtures (small concentration gradients)

Figure 29 shows a schema of the apparatus used to prepare the desired heterogeneous gas mixture in a 4-inch diameter, 20 liter Plexiglas cylinder (C). An experiment is conducted in the following manner. The desired air flow is first adjusted by means of flowmeter (B) and the electrical circuit is balanced such that a zero reading is obtained on the 25 mv null meter. The calibrated linear potentiometer (E) is rotated until its voltage output read on the nullmeter is equal to the output of the bridge circuit which corresponds to a 5 percent methane-air mixture. The methane flow is then increased until a zero reading is again obtained on the nullmeter. The methane-air mixture flowing into the chamber now contains 5 percent methane. The 1/3 rpm geared motor is then started and rotates the potentiometer (E). Then, in order to maintain a zero reading on the nullmeter, it is necessary to increase the methane flow rate manually; in this manner the methane concentration in the gas mixture is increased linearly with time. The whole apparatus has been adjusted so that in the time required to completely fill the tube with the heterogeneous gas mixture (2 minutes) the methane concentration increases from 5 to 20 volume percent. After the tube has been filled, the gases are ignited with a hot wire wrapped with guncotton and propagation of the flame up the tube is photographed with a 16 mm motion picture camera (D) operated at 64 frames per second.

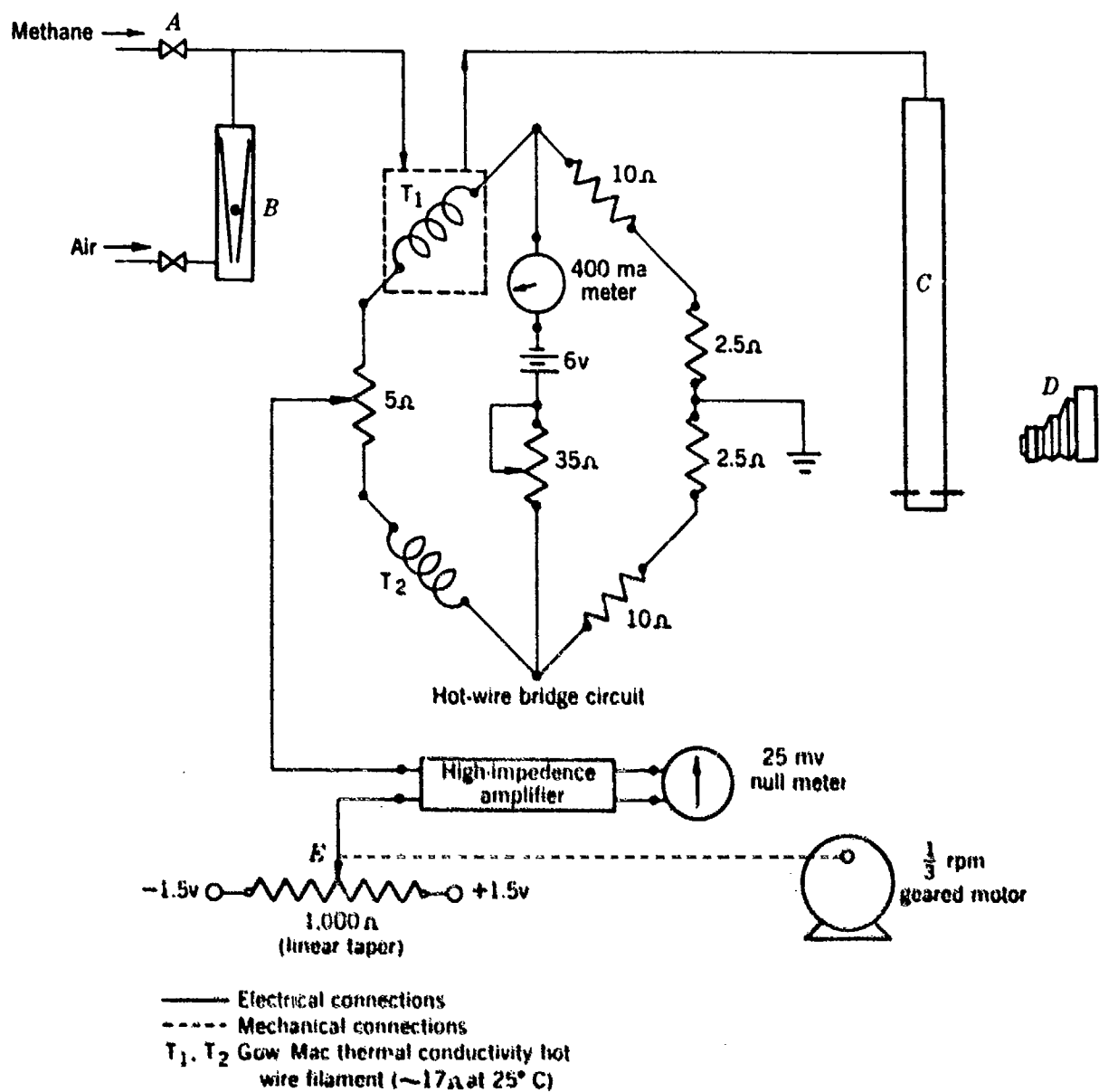


Figure 29. - Schema of apparatus used to prepare heterogeneous methane-air mixtures.

#### APPENDIX IV - Flowing Stratified Mixtures

The 67-foot gallery (tunnel) shown in Figure 30 is formed from a 1/2-inch thick steel cylinder. The flowmeter (M) and thermal conductivity gas analyzer (T) are located at the side of the gallery for convenience. Ventilation air flow is determined by the fan speed and screen size. Natural gas is introduced into the gallery roof through the flowmeter (M) and the gas diffuser (D). Gas concentrations in the gallery are determined at four stations (1,2,3,4) by use of sampling probe (S) and gas analyzer (T); pump (P) withdraws samples continuously. The sampling probe can be positioned vertically at any of the four stations. The natural gas roof layer can be ignited at either  $I_1$  or  $I_2$ ; the radiant energy from the flame is detected by photo-diodes located at positions 5, 6, 7 and 8; these observe an area approximately 2.3 ft.<sup>2</sup> at the gallery roof. The signals from these units are amplified and then recorded on a Brush direct-inking oscillograph.

A motion picture camera located approximately 6 feet from the open end of the gallery is used to record the motion of the flame.

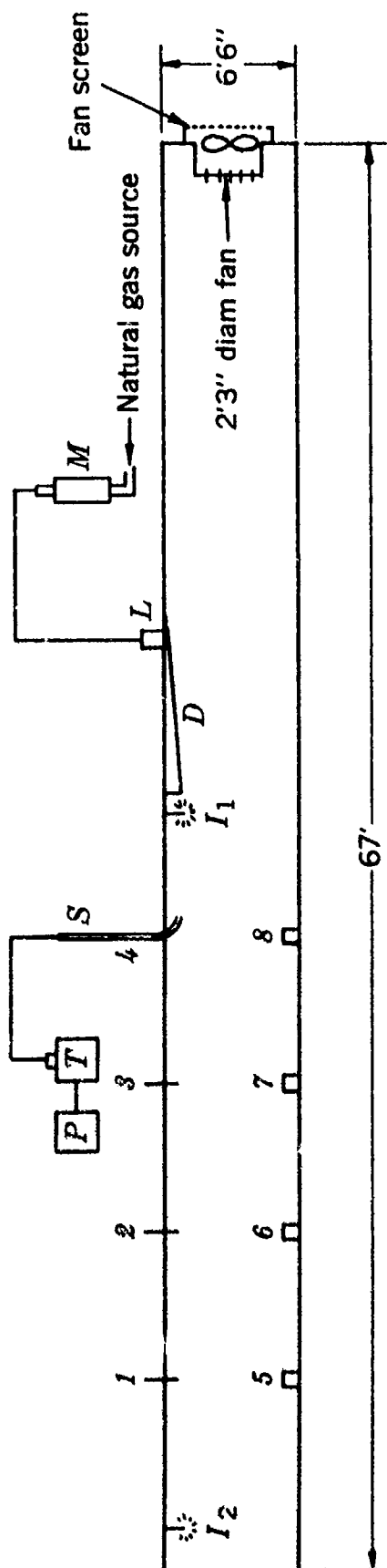


Figure 30. - Gallery and associated apparatus used for flammability studies of flowing mixtures.



## APPENDIX V - Acceleration Apparatus

Figure 31 shows a photograph of the acceleration apparatus used to conduct autoignition tests under increased accelerational fields. The apparatus consists of two electrically heated 6-inch diameter stainless steel spheres (A) attached to the extremities of a 6-foot length of 1/4-inch pipe. The steel spheres are made of two flanged hemispheres so as to provide ready access for cleaning. Rotating the pipe in a horizontal plane around its center by means of a geared electric motor subjects the spheres to a radial acceleration field. Measured volumes of liquid fuel are contained in two glass syringes located inside the brass containers (B). A 3-1/2-foot length of stainless steel hypodermic tubing (C) attached to the end of the glass syringes protruding from the top of the brass containers is used to convey the liquid fuel from the syringe into the steel spheres. The fuel is injected into the spheres pneumatically by use of the high pressure reservoir (D) and remotely controlled solenoid valve (E). An armature (F) and carbon brushes provide electrical connection to the recording thermocouples (H), to the rotating spheres for controlling the temperature of the heating mantle (J), and to the electric solenoid. There are two sets of thermocouples connected to the sphere, one is attached directly to the exterior wall of each sphere and is used for temperature control, the other is located at the center of the sphere and when connected to a millivolt recorder gives an indication of ignition. An experiment is conducted by (1) heating the spheres to the desired temperature, (2) filling the syringe with the required quantity of fuel, and (3) loading the compressed air reservoir with 40 psig of air. A controlled-speed motor (located behind the operator shown in photograph) gradually increases the rotational speed of the spheres to the desired value at which speed the solenoid is actuated and the compressed air from the reservoir rushes in behind the syringe forcing the liquid fuel into the test spheres. A recording millivoltmeter records the temperature of the thermocouples located within the spheres. An ignition is evidenced by a sharp change in temperature.



Figure 31. - Acceleration apparatus.



Aeronautical Systems Division, AF Aero-Propulsion Laboratory, Hazards and Fluid Support Branch, Wright-Patterson AFB, Ohio. Rpt No. ASD-TR-61-278, Sup 2. REVIEW OF FIRE AND EXPLOSION HAZARDS OF FLIGHT VEHICLE COMBUSTIBLES. Interim report, June 1963, 49pp., incl illus., 13 refs.

#### Unclassified Report

This is the third in a series of reports on the fire and explosion hazards associated with combustibles and other gases likely to be found in aircraft and missile systems. It presents theoretical and experimental results on homogeneous and heterogeneous mix-

( over )

tures in air. Two pressure peaks were observed in venting hydrogen-air mixtures into a low pressure atmosphere. When venting a fire above a liquid pool under the same conditions, the liquid regression rate and flame size were found to increase. Molecular diffusion appears to be the chief factor in establishing the position of the lower limit of flammability of both lighter-than-air and heavier-than-air combustible, quiescent, gas layers; the position of the upper limit cannot be predicted by considering molecular diffusion alone. The ratio of the work done against the gravitational force to that done by the turbulent stresses is useful in analyzing mixing processes in flowing, layered systems. The gravitational filed strength also appears to affect the time delay before ignition of a combustible vapor in air.

1. Hazards, fire & explosion
2. Flight Vehicles
3. Flammability
- I. AFSC Project 6075, Task 607504
- II. Contract AF(33-616) 60-8

#### III. Bureau of Mines, U. S. Department of the Interior

- IV. Henry E. Perlee, Israel Liebman, Michael G. Zabetakis
- V. Aval fr OTS
- VI. In ASTIA collection

Aeronautical Systems Division, AF Aero-Propulsion Laboratory, Hazards and Fluid Support Branch, Wright-Patterson AFB, Ohio. Rpt No. ASD-TR-61-278, Sup 2. REVIEW OF FIRE AND EXPLOSION HAZARDS OF FLIGHT VEHICLE COMBUSTIBLES. Interim report, June 1963, 49pp., incl illus., 13 refs.

#### Unclassified Report

This is the third in a series of reports on the fire and explosion hazards associated with combustibles and other gases likely to be found in aircraft and missile systems. It presents theoretical and experimental results on homogeneous and heterogeneous mix-

( over )

tures in air. Two pressure peaks were observed in venting hydrogen-air mixtures into a low pressure atmosphere. When venting a fire above a liquid pool under the same conditions, the liquid regression rate and flame size were found to increase. Molecular diffusion appears to be the chief factor in establishing the position of the lower limit of flammability of both lighter-than-air and heavier-than-air combustible, quiescent, gas layers; the position of the upper limit cannot be predicted by considering molecular diffusion alone. The ratio of the work done against the gravitational force to that done by the turbulent stresses is useful in analyzing mixing processes in flowing, layered systems. The gravitational filed strength also appears to affect the time delay before ignition of a combustible vapor in air.

1. Hazards, fire & explosion
2. Flight Vehicles
3. Flammability
- I. AFSC Project 6075, Task 607504
- II. Contract AF(33-616) 60-8
- III. Bureau of Mines, U. S. Department of the Interior
- IV. Henry E. Perlee, Israel Liebman, Michael G. Zabetakis
- V. Aval fr OTS
- VI. In ASTIA collection